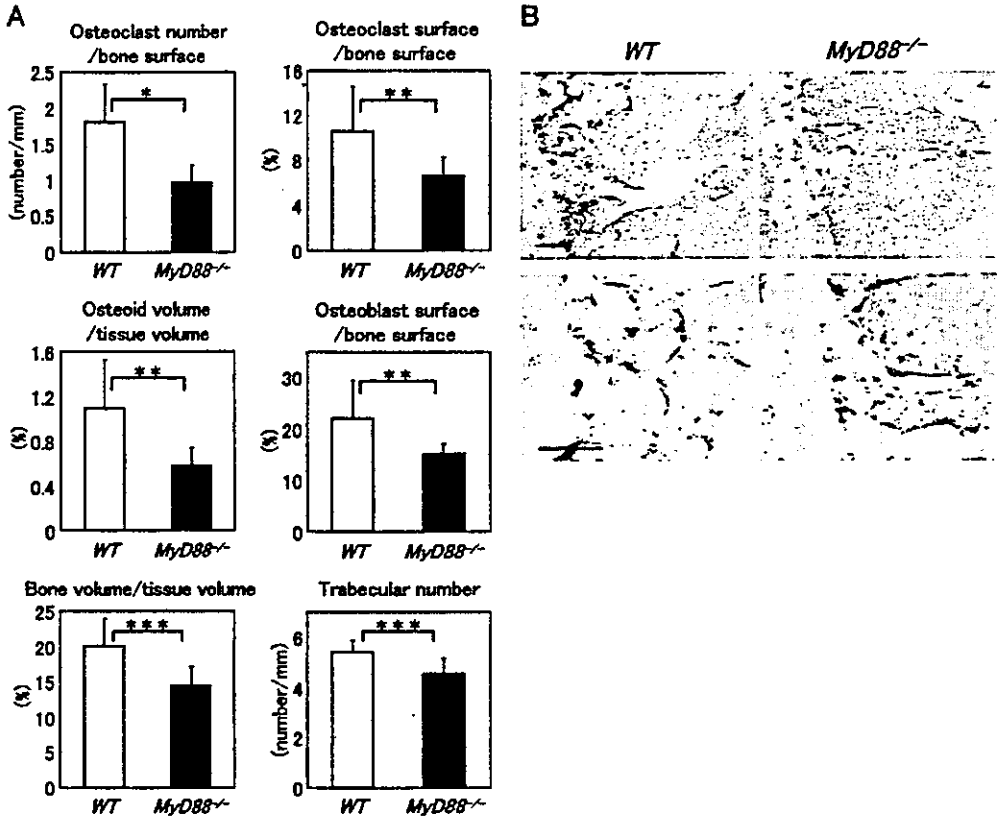

Figure 7. Histomorphometric analysis of vertebrae in WT and MyD88$^{-/-}$ mice. (A) Seven male MyD88$^{-/-}$ and WT (14-wk-old) mice each were killed for bone histomorphometric analysis. Vertebrae were removed from the mice, fixed in 70% ethanol, and embedded in glycol-methacrylate without decalcification. Sections were prepared and stained with Villanueva Goldner to discriminate between mineralized and unmineralized bone and to identify cellular components. Quantitative histomorphometric analysis was done in a double-blind fashion. Values were expressed as the mean ± SD of seven mice. Statistical analysis was performed using Student's *t* test. Significant difference between WT and MyD88$^{-/-}$ mice (*, $P < 0.005$; **, $P < 0.05$; ***, $P < 0.01$). (B) Histological evaluation (double staining of TRAP and methylgreen) of femoral trabecular bones obtained from male MyD88$^{-/-}$ and WT (12-wk-old) mice. TRAP positive osteoclasts appeared dark red. Arrowheads indicate osteoblasts along the bone surface. Bars, 500 μm.

all stimulated osteoclast formation in cocultures of osteoblasts and hemopoietic cells obtained from WT and TRIF$^{-/-}$ mice, but not from MyD88$^{-/-}$ mice (Figs. 1 and 4). Osteoclast precursors from MyD88$^{-/-}$ mice and WT mice similarly differentiated into osteoclasts in response to RANKL plus M-CSF, but the extent of osteoclast formation induced by $1,25(OH)_2D_3$ plus PGE_2 in the MyD88$^{-/-}$ mice was always significantly less than that in wild-type cocultures (Fig. 1). This suggests that MyD88 is involved in osteoblast function including the support of osteoclasts in response to $1,25(OH)_2D_3$ plus PGE_2. LPS, diacyl lipopeptide, and IL-1α stimulated expression of RANKL mRNA in WT and TRIF$^{-/-}$ osteoblasts, but not MyD88$^{-/-}$ osteoblasts (Figs. 2 and 4). These results suggest that RANKL expression in osteoblasts through MyD88-mediated signals is a key step in osteoclast formation induced by LPS, diacyl lipopeptide, and IL-1 (Fig. 8).

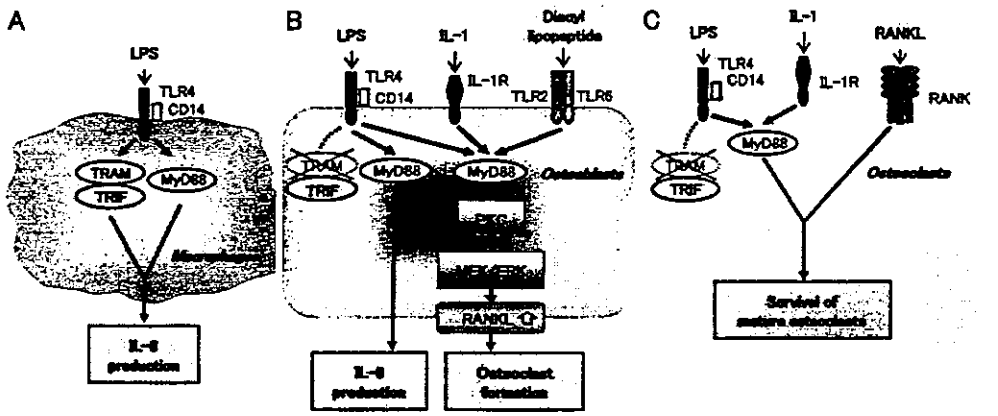

Figure 8. Roles of MyD88 and TRAM–TRIF signaling pathways in macrophages, osteoblasts, and osteoclasts exposed to LPS, IL-1, diacyl lipopeptide, and RANKL. (A) Role of MyD88- and TRAM–TRIF-mediated signaling in IL-6 production in macrophages. Macrophages express CD14 and TLR4. Both MyD88-dependent and TRAM–TRIF-dependent pathways mediated by TLR4 were essential for IL-6 production in macrophages. (B) Roles of MyD88-mediated signals in IL-6 production and osteoclast formation in osteoblasts. Osteoblasts express CD14, TLR2, TLR4, TLR6, and IL-1R. LPS stimulates IL-6 production through MyD88 signaling. LPS, IL-1, and diacyl lipopeptide stimulate RANKL expression in osteoblasts through the respective receptor systems. TLR- and IL-1R–induced RANKL mRNA expression in osteoblasts is mediated through MyD88 signaling followed by PKC and MEK/ERK signaling. (C) Role of MyD88-mediated signals in osteoclast function. Mature osteoclasts express CD14, TLR4, and IL-1R as well as RANK. LPS, IL-1, and RANKL stimulate the survival of osteoclasts through TLR4, IL-1R, and RANK, respectively. MyD88 is involved in the survival of osteoclasts supported by LPS and IL-1, but not by RANKL.

LPS and IL-1α stimulated phosphorylation of ERK1/2 in WT osteoblasts, but not MyD88$^{-/-}$ osteoblasts (Fig. 3). The elevated calcium concentration (5 mM) in the culture medium stimulated both phosphorylation of ERK1/2 and RANKL mRNA expression in WT and MyD88$^{-/-}$ osteoblasts. This calcium concentration did not appear to be toxic to the cells. A serine threonine kinase, Cot, also known as tumor progression locus 2 (Tpl2), has been shown to be an essential kinase in LPS-induced TNFα production in mouse macrophages (34, 35). Cot/Tpl2 activated ERK, but not JNK and p38 MAPK, in the LPS-treated macrophages. It was reported that both RANKL mRNA induction and ERK activation by LPS were markedly reduced in osteoblasts prepared from Cot/Tpl2-deficient mice (36). These results suggest that LPS-induced RANKL mRNA expression is mediated through MyD88 followed by PKC and MEK/ERK signals rather than JNK and p38 MAPK signals (Fig. 8).

We reported previously that osteoclasts formed in vitro expressed TLR4 and CD14, and LPS directly supported the survival and stimulated the dentine-resorbing activity of osteoclasts (32). Takami et al. (33) showed that mouse bone marrow macrophages expressed all known TLRs (TLR1–TLR9), but mouse osteoclasts expressed only TLR2 and TLR4. Consistent with these findings, LPS and IL-1α but not diacyl lipopeptide (a ligand for the TLR2 plus TLR6 complex) stimulated the survival of osteoclasts derived from WT and TRIF$^{-/-}$ mice (Fig. 5). The survival of osteoclasts from MyD88$^{-/-}$ mice was supported by RANKL, but not by LPS and IL-1α. These results suggest that MyD88 but not TRIF is involved in IL-1R– and TLR4-mediated signaling in the survival of osteoclasts. MyD88 and RANK are shown to associate with TNF receptor-associated factor 6 to induce their signals in target cells. TNF receptor-associated factor 6 appears to be a common signaling molecule downstream of MyD88 and RANK in osteoclasts.

Recent studies using TRIF$^{-/-}$ mice showed the essential role of TRIF in the MyD88-independent pathways of TLR3 and TLR4 signaling (17, 18). TRAM was shown to be involved in the TLR4-mediated TRIF-signaling pathway in the innate immune response to LPS (19, 20). Consistent with previous findings, TRIF$^{-/-}$ macrophages abolished the response to LPS in IL-6 production (Fig. 4). However, surprisingly, TRIF$^{-/-}$ osteoblasts and TRIF$^{-/-}$ osteoclasts responded to LPS as those from WT mice did. Osteoblasts and osteoclasts expressed TRIF but not TRAM, suggesting that TRAM expression is required for TRIF-mediated action in osteoblasts and osteoclasts (Fig. 8). Our results also suggest that TRAM may be an important key adaptor in the TLR4-mediated pathway of cell-specific functions.

At present, it is unknown why immune cells such as macrophages and B cells required both MyD88 and TRIF signaling in response to LPS. We reported previously that LPS stimulated the production of proinflammatory cytokines such as IL-1β, TNF-α, and IL-6 in bone marrow macrophages but not in osteoclasts (32). Thus, osteoclasts respond to LPS through TLR4, but the characteristics of osteoclasts are quite different from those of their precursors, bone marrow macrophages. These results suggest that TRIF is important for the function of immune cells, but not that of nonimmune cells such as osteoblasts and osteoclasts. Loss of immune responsiveness to LPS in osteoclasts must be a requirement for performing essential roles in physiological bone turnover. Further studies will elucidate the significance of the requirement of TRAM–TRIF signals in immune cells.

MyD88$^{-/-}$ mice exhibited a significant decrease in trabecular bone volume and trabecular number in vertebrae, although no significant differences in body size and shape were observed between MyD88$^{-/-}$ and WT mice. Not only bone resorption–related parameters but also bone formation–related parameters were significantly decreased in MyD88$^{-/-}$ mice in comparison with WT mice (Fig. 7). Mice deficient in bone matrix proteins such as osteonectin and biglycan similarly developed profound osteopenia with a decrease of bone formation and resorption (37–39). Deficiency of OPG in mice induced severe osteoporosis caused by enhanced bone resorption, but accelerated bone formation was also observed in these mice (27, 40). These findings suggest that bone formation is tightly coupled with bone resorption.

In conclusion, MyD88 but not TRIF plays essential roles in RANKL expression in osteoblasts in response to IL-1 and TLR ligands. MyD88 is also a key molecule for osteoclast function induced by IL-1 and LPS. MyD88$^{-/-}$ mice exhibit osteopenia with reduced bone resorption and bone formation. Thus, MyD88-mediated signaling plays important roles not only in bone resorption induced by inflammatory diseases but also in ordinary bone metabolism. Further studies are necessary to clarify the physiological and pathological significance of MyD88 signals in bone resorption and bone formation.

We thank Drs. H. Ozawa and Y. Nakamichi for helpful discussion and technical assistance. We also thank Ms. A. Ito and Dr. N. Yamamoto for technical assistance in bone histomorphometry.

This work was supported in part by Grants-in-Aid 13557155, 14370599, 15390565, 15390641, and 15659445 and AGU High-Tech Research Center Project from the Ministry of Education, Culture, Sports, Science and Technology of Japan, and by a grant from the Kato Memorial Bioscience Foundation.

The authors have no conflicting financial interests.

Submitted: 7 April 2004
Accepted: 28 July 2004

References

1. Takahashi, N., N. Udagawa, M. Takami, and T. Suda. 2002. Cells of bone: osteoclast generation. *In* Principles of Bone Biology Second Edition. J.P. Bilezikian, L.G. Raisz, and G.A. Rodan, editors. Academic Press, San Diego, CA. 109–126.
2. Suda, T., N. Takahashi, N. Udagawa, E. Jimi, M.T. Gillespie, and T.J. Martin. 1999. Modulation of osteoclast differentiation and function by the new members of the tumor necrosis factor receptor and ligand families. *Endocr. Rev.*

20:345–357.
3. Boyle, W.J., W.S. Simonet, and D.L. Lacey. 2003. Osteoclast differentiation and activation. *Nature*. 423:337–342.
4. Hofbauer, L.C., S. Khosla, C.R. Dunstan, D.L. Lacey, W.J. Boyle, and B.L. Riggs. 2000. The roles of osteoprotegerin and osteoprotegerin ligand in the paracrine regulation of bone resorption. *J. Bone Miner. Res.* 15:2–12.
5. Arron, J.R., and Y. Choi. 2000. Bone versus immune system. *Nature*. 408:535–536.
6. Udagawa, N., N. Takahashi, H. Yasuda, A. Mizuno, K. Itoh, Y. Ueno, T. Shinki, M.T. Gillespie, T.J. Martin, K. Higashio, and T. Suda. 2000. Osteoprotegerin produced by osteoblasts is an important regulator in osteoclast development and function. *Endocrinology*. 141:3478–3484.
7. Nair, S.P., S. Meghji, M. Wilson, K. Reddi, P. White, and B. Henderson. 1996. Bacterially induced bone destruction: mechanisms and misconceptions. *Infect. Immun.* 64:2371–2380.
8. Yeh, W.C., and N.J. Chen. 2003. Immunology: another toll road. *Nature*. 424:736–737.
9. Akira, S. 2003. Toll-like receptor signaling. *J. Biol. Chem.* 278:38105–38108.
10. Fujita, M., T. Into, M. Yasuda, T. Okusawa, S. Hamahira, Y. Kuroki, A. Eto, T. Nisizawa, M. Morita, and K.I. Shibata. 2003. Involvement of leucine residues at positions 107, 112, and 115 in a leucine-rich repeat motif of human Toll-like receptor 2 in the recognition of diacylated lipoproteins and lipopeptides and *Staphylococcus aureus* peptidoglycans. *J. Immunol.* 171:3675–3683.
11. Nakamura, J., K. Shibata, A. Hasebe, T. Into, T. Watanabe, and N. Ohata. 2002. Signaling pathways induced by lipoproteins derived from *Mycoplasma salivarium* and a synthetic lipopeptide (FSL-1) in normal human gingival fibroblasts. *Microbiol. Immunol.* 46:151–158.
12. Adachi, O., T. Kawai, K. Takeda, M. Matsumoto, H. Tsutsui, M. Sakagami, K. Nakanishi, and S. Akira. 1998. Targeted disruption of the MyD88 gene results in loss of IL-1- and IL-18-mediated function. *Immunity*. 9:143–150.
13. Kawai, T., O. Adachi, T. Ogawa, K. Takeda, and S. Akira. 1999. Unresponsiveness of MyD88-deficient mice to endotoxin. *Immunity*. 11:115–122.
14. Takeuchi, O., A. Kaufmann, K. Grote, T. Kawai, K. Hoshino, M. Morr, P.F. Muhlradt, and S. Akira. 2000. Preferentially the R-stereoisomer of the mycoplasmal lipopeptide macrophage-activating lipopeptide-2 activates immune cells through a toll-like receptor 2- and MyD88-dependent signaling pathway. *J. Immunol.* 164:554–557.
15. Kaisho, T., O. Takeuchi, T. Kawai, K. Hoshino, and S. Akira. 2001. Endotoxin-induced maturation of MyD88-deficient dendritic cells. *J. Immunol.* 166:5688–5694.
16. Yamamoto, M., S. Sato, K. Mori, K. Hoshino, O. Takeuchi, K. Takeda, and S. Akira. 2002. A novel Toll/IL-1 receptor domain-containing adapter that preferentially activates the IFN-β promoter in the Toll-like receptor signaling. *J. Immunol.* 169:6668–6672.
17. Yamamoto, M., S. Sato, H. Hemmi, K. Hoshino, T. Kaisho, H. Sanjo, O. Takeuchi, M. Sugiyama, M. Okabe, K. Takeda, and S. Akira. 2003. Role of adaptor TRIF in the MyD88-independent toll-like receptor signaling pathway. *Science*. 301:640–643.
18. Hoebe, K., X. Du, P. Georgel, E. Janssen, K. Tabeta, S.O. Kim, J. Goode, P. Lin, N. Mann, S. Mudd, et al. 2003. Identification of Lps2 as a key transducer of MyD88-independent TIR signalling. *Nature*. 424:743–748.
19. Yamamoto, M., S. Sato, H. Hemmi, S. Uematsu, K. Hoshino, T. Kaisho, O. Takeuchi, K. Takeda, and S. Akira. 2003. TRAM is specifically involved in the Toll-like receptor 4-mediated MyD88-independent signaling pathway. *Nat. Immunol.* 4:1144–1150.
20. Fitzgerald, K.A., D.C. Rowe, B.J. Barnes, D.R. Caffrey, A. Visintin, E. Latz, B. Monks, P.M. Pitha, and D.T. Golenbock. 2003. LPS-TLR4 signaling to IRF-3/7 and NF-κB involves the toll adapters TRAM and TRIF. *J. Exp. Med.* 198: 1043–1055.
21. Kondo, A., Y. Koshihara, and A. Togari. 2001. Signal transduction system for interleukin-6 synthesis stimulated by lipopolysaccharide in human osteoblasts. *J. Interferon Cytokine Res.* 21:943–950.
22. Hoshino, K., O. Takeuchi, T. Kawai, H. Sanjo, T. Ogawa, Y. Takeda, K. Takeda, and S. Akira. 1999. Toll-like receptor 4 (TLR4)-deficient mice are hyporesponsive to lipopolysaccharide: evidence for TLR4 as the Lps gene product. *J. Immunol.* 162:3749–3752.
23. Shibata, K., A. Hasebe, T. Into, M. Yamada, and T. Watanabe. 2000. The N-terminal lipopeptide of a 44-kDa membrane-bound lipoprotein of *Mycoplasma salivarium* is responsible for the expression of intercellular adhesion molecule-1 on the cell surface of normal human gingival fibroblasts. *J. Immunol.* 165:6538–6544.
24. Suda, T., E. Jimi, I. Nakamura, and N. Takahashi. 1997. Role of 1α,25-dihydroxyvitamin D_3 in osteoclast differentiation and function. *Methods Enzymol.* 282:223–235.
25. Takami, M., N. Takahashi, N. Udagawa, C. Miyaura, K. Suda, J.T. Woo, T.J. Martin, K. Nagai, and T. Suda. 2000. Intracellular calcium and protein kinase C mediate expression of receptor activator of nuclear factor-κB ligand and osteoprotegerin in osteoblasts. *Endocrinology*. 141:4711–4719.
26. Parfitt, A.M., M.K. Drezner, F.H. Glorieux, J.A. Kanis, H. Malluche, P.J. Meunier, S.M. Ott, and R.R. Recker. 1987. Bone histomorphometry: standardization of nomenclature, symbols, and units. Report of the ASBMR Histomorphometry Nomenclature Committee. *J. Bone Miner. Res.* 2:595–610.
27. Mizuno, A., N. Amizuka, K. Irie, A. Murakami, N. Fujise, T. Kanno, Y. Sato, N. Nakagawa, H. Yasuda, S. Mochizuki, et al. 1998. Severe osteoporosis in mice lacking osteoclastogenesis inhibitory factor/osteoprotegerin. *Biochem. Biophys. Res. Commum.* 247:610–615.
28. Nakamura, M., N. Udagawa, S. Matsuura, M. Mogi, H. Nakamura, H. Horiuchi, N. Saito, B.Y. Hiraoka, Y. Kobayashi, K. Takaoka, et al. 2003. Osteoprotegerin regulates bone formation through a coupling mechanism with bone resorption. *Endocrinology*. 144:5441–5449.
29. Suda, K., N. Udagawa, N. Sato, M. Takami, K. Itoh, J.-T. Woo, N. Takahashi, and K. Nagai. 2004. Suppression of osteoprotegerin expression by prostaglandin E2 is crucially involved in lipopolysaccharide-induced osteoclast formation. *J. Immunol.* 172:2504–2510.
30. Kikuchi, T., T. Matsuguchi, N. Tsuboi, A. Mitani, S. Tanaka, M. Matsuoka, G. Yamamoto, T. Hishikawa, T. Noguchi, and Y. Yoshikai. 2001. Gene expression of osteoclast differentiation factor is induced by lipopolysaccharide in mouse osteoblasts via Toll-like receptors. *J. Immunol.* 166: 3574–3579.
31. Jimi, E., I. Nakamura, L.T. Duong, T. Ikebe, N. Takahashi, G.A. Rodan, and T. Suda. 1999. Interleukin 1 induces multinucleation and bone-resorbing activity of osteoclasts in the absence of osteoblasts/stromal cells. *Exp. Cell Res.* 247:

84–93.
32. Itoh, K., N. Udagawa, K. Kobayashi, K. Suda, X. Li, M. Takami, N. Okahashi, T. Nishihara, and N. Takahashi. 2003. Lipopolysaccharide promotes the survival of osteoclasts via Toll-like receptor 4, but cytokine production of osteoclasts in response to lipopolysaccharide is different from that of macrophages. *J. Immunol.* 170:3688–3695.
33. Takami, M., N. Kim, J. Rho, and Y. Choi. 2002. Stimulation by toll-like receptors inhibits osteoclast differentiation. *J. Immunol.* 169:1516–1523.
34. Waterfield, M.R., M. Zhang, L.P. Norman, and S.C. Sun. 2003. NF-κB1/p105 regulates lipopolysaccharide-stimulated MAP kinase signaling by governing the stability and function of the Tpl2 kinase. *Mol. Cell.* 11:685–694.
35. Barton, G.M., and R. Medzhitov. 2003. Toll-like receptor signaling pathways. *Science.* 300:1524–1525.
36. Kikuchi, T., Y. Yoshikai, J. Miyoshi, M. Katsuki, T. Musikacharoen, A. Mitani, S. Tanaka, T. Noguchi, and T. Matsuguchi. 2003. Cot/Tpl2 is essential for RANKL induction by lipid A in osteoblasts. *J. Dent. Res.* 82:546–550.
37. Gilmour, D.T., G.J. Lyon, M.B. Carlton, J.R. Sanes, J.M. Cunningham, J.R. Anderson, B.L. Hogan, M.J. Evans, and W.H. Colledge. 1998. Mice deficient for the secreted glycoprotein SPARC/osteonectin/BM40 develop normally but show severe age-onset cataract formation and disruption of the lens. *EMBO J.* 17:1860–1870.
38. Delany, A.M., M. Amling, M. Priemel, C. Howe, R. Baron, and E. Canalis. 2000. Osteopenia and decreased bone formation in osteonectin-deficient mice. *J. Clin. Invest.* 105:1325.
39. Xu, T., P. Bianco, L.W. Fisher, G. Longenecker, E. Smith, S. Goldstein, J. Bonadio, A. Boskey, A.M. Heegaard, B. Sommer, et al. 1998. Targeted disruption of the biglycan gene leads to an osteoporosis-like phenotype in mice. *Nat. Genet.* 20:78–82.
40. Bucay, N., I. Sarosi, C.R. Dunstan, S. Morony, J. Tarpley, C. Capparelli, S. Scully, H.L. Tan, W. Xu, D.L. Lacey, et al. 1998. osteoprotegerin-deficient mice develop early onset osteoporosis and arterial calcification. *Genes Dev.* 12:1260–1268.

THE JOURNAL OF BIOLOGICAL CHEMISTRY
Vol. 280, No. ??, Issue of ???? ??, pp. 1–xxx, 2005
Printed in U.S.A.
© 2005 by The American Society for Biochemistry and Molecular Biology, Inc.

Prostaglandin E_2 Enhances Osteoclastic Differentiation of Precursor Cells through Protein Kinase A-dependent Phosphorylation of TAK1*

Received for publication, September 29, 2004, and in revised form, December 14, 2004
Published, JBC Papers in Press, January 12, 2005, DOI 10.1074/jbc.M411189200

Yasuhiro Kobayashi‡, Toshihide Mizoguchi‡, Ikuko Take‡§, Saburo Kurihara§, Nobuyuki Udagawa¶, and Naoyuki Takahashi‡‖

From the ‡Institute for Oral Science, the §Department of Orthodontics and the ¶Department of Biochemistry, Matsumoto Dental University, 1780 Hiro-oka Gobara, Shiojiri, Nagano 399-0781, Japan

Prostaglandin E_2 (PGE_2) synergistically enhances the receptor activator for NF-κB ligand (RANKL)-induced osteoclastic differentiation of the precursor cells. Here we investigated the mechanisms of the stimulatory effect of PGE_2 on osteoclast differentiation. PGE_2 enhanced osteoclastic differentiation of RAW264.7 cells in the presence of RANKL through EP2 and EP4 prostanoid receptors. RANKL-induced degradation of IκBα and phosphorylation of p38 MAPK and c-Jun N-terminal kinase in RAW264.7 cells were up-regulated by PGE_2 in a cAMP-dependent protein kinase A (PKA)-dependent manner, suggesting that EP2 and EP4 signals cross-talk with RANK signals. Transforming growth factor β-activated kinase 1 (TAK1), an important MAPK kinase kinase in several cytokine signals, possesses a PKA recognition site at amino acids 409–412. PKA directly phosphorylated TAK1 in RAW264.7 cells transfected with wild-type TAK1 but not with the $Ser^{412} \rightarrow Ala$ mutant TAK1. $Ser^{412} \rightarrow Ala$ TAK1 served as a dominant-negative mutant in PKA-enhanced degradation of IκBα, phosphorylation of p38 MAPK, and PGE_2-enhanced osteoclastic differentiation in RAW264.7 cells. Furthermore, forskolin enhanced tumor necrosis factor α-induced IκBα degradation, p38 MAPK phosphorylation, and osteoclastic differentiation in RAW264.7 cells. $Ser^{412} \rightarrow Ala$ TAK1 abolished the stimulatory effects of forskolin on those cellular events induced by tumor necrosis factor α. $Ser^{412} \rightarrow Ala$ TAK1 also inhibited the forskolin-induced up-regulation of interleukin 6 production in RAW264.7 cells treated with lipopolysaccharide. These results suggest that the phosphorylation of the Ser^{412} residue in TAK1 by PKA is essential for cAMP/PKA-induced up-regulation of osteoclastic differentiation and cytokine production in the precursor cells.

AQ: A

Osteoclasts are bone-resorbing multinucleated cells derived from the monocyte-macrophage lineage (1–3). The differentiation and activation of osteoclasts are tightly regulated by osteoblasts or bone marrow-derived stromal cells (4–6). Osteoblasts express two cytokines essential for osteoclast differentiation: receptor activator of NF-κB ligand (RANKL)[1] and macrophage colony-stimulating factor (M-CSF) (7, 8). The expression of RANKL in osteoblasts is up-regulated by several osteotropic factors such as interleukin 11 (IL-11), parathyroid hormone, 1α,25-dihydroxyvitamin D_3, IL-1, and lipopolysaccharide (LPS) (7, 9). Osteoclast precursors differentiate into mature osteoclasts in the presence of RANKL and M-CSF (10, 11). Recent studies have shown that mouse macrophage-like RAW264.7 cells can differentiate into osteoclasts in response to RANKL even in the absence of M-CSF (12). We and others (13–15) have reported that tumor necrosis factor α (TNFα) stimulates osteoclastic differentiation from bone marrow macrophages through a mechanism independent of the RANKL-RANK interaction. RAW264.7 cells also differentiate into osteoclasts in response to TNFα even in the absence of RANKL (16). Thus, two cytokines, RANKL and TNFα, induce the differentiation of osteoclasts from the precursor cells of the monocyte-macrophage lineage.

Fn1

PGE_2 has been proposed to be a potent stimulator of osteoclastic bone resorption involved in inflammatory diseases such as rheumatoid arthritis and osteomyelitis (17–20). Like other osteotropic factors, PGE_2 stimulates RANKL expression in osteoblasts (21, 22). The functions of PGE_2 in the target cells are mediated by four different G protein-coupled receptor subtypes, EP1, EP2, EP3, and EP4 (23, 24). The signal of EP1 increases intracellular Ca^{2+} and activates protein kinase C. EP2 and EP4 activate G_s, which stimulates cAMP generation, followed by the activation of cAMP-dependent protein kinase A (PKA), in the target cells. Conversely, EP3 acts via G_i to inhibit cAMP generation. Among these PGE_2 receptor subtypes, EP4 mainly mediates PGE_2-induced RANKL expression in osteoblasts (21, 25). In addition, PGE_2 synergistically stimulates the differentiation of bone marrow macrophages into osteoclasts

* This work was supported in part by Grants-in-aid 12137209, 13470394, 14207075, 14370599, 15390565, and 15390641 from the Ministry of Education, Culture, Sports, Science, and Technology of Japan. The costs of publication of this article were defrayed in part by the payment of page charges. This article must therefore be hereby marked "*advertisement*" in accordance with 18 U.S.C. Section 1734 solely to indicate this fact.

‖ To whom correspondence should be addressed: Institute for Oral Science, Matsumoto Dental University, 1780 Hiro-oka Gobara, Shiojiri, Nagano 399-0781, Japan. Tel.: 81-263-51-2135; Fax: 81-263-51-2223; E-mail: takahashinao@po.mdu.ac.jp.

[1] The abbreviations used are: RANKL, receptor activator for NF-κB ligand; IL, interleukin; PGE_2, prostaglandin E_2; NF-κB, nuclear factor-κB; RANK, receptor activator of NF-κB; MAPK, mitogen-activated protein kinase; MAPKKK, MAPK kinase kinase; MAPKK, MAPK kinase; PKA, protein kinase A; TNF, tumor necrosis factor; TRAF, TNF receptor-associated factor; JNK, c-Jun N-terminal kinase; ERK, extracellular signal-regulated kinase; M-CSF, macrophage-colony-stimulating factor; TGF-β, transforming growth factor-β; TAK1, TGF-β-activated kinase 1; TAB, TAK1-binding protein; CT, calcitonin; IBMX, 3-isobutyl-1-methylxanthine; G3PDH, glyceraldehyde-3-phosphate dehydrogenase; LPS, lipopolysaccharide; TLR, toll-like receptor; MyD88, myeloid differentiation factor 88; TRIF, Toll-IL-1 receptor domain-containing adaptor-inducing interferon-β; RT, reverse transcription; α-MEM, α-MEM minimum Eagle's medium; FBS, fetal bovine serum; ELISA, enzyme-linked immunosorbent assay; BMMφ, bone marrow-derived macrophages; Bt_2cAMP, dibutyryl cyclic AMP; TRAP, tartrate-resistant acid phosphatase; WT, wild type.

induced by RANKL and M-CSF (26, 27). Thus, PGE_2 stimulates osteoclastic bone resorption through the following two different pathways: the induction of RANKL expression in osteoblasts, and the direct enhancement of RANKL-induced differentiation of osteoclast precursor cells into osteoclasts. The mechanism of the synergistic effect of PGE_2 on the RANKL-induced osteoclastic differentiation of precursor cells has not yet been explained.

When RANKL binds to RANK, the receptor for RANKL, TNF receptor-associated factor 1 (TRAF1), TRAF2, TRAF3, TRAF5, and TRAF6 interact with the cytoplasmic tail of RANK (28, 29). The ligand-dependent interaction of TRAFs with RANK induces activation of nuclear factor-κB (NF-κB), c-Jun N-terminal kinase (JNK), p38 mitogen-activated protein kinase (MAPK), and extracellular signal-regulated kinase (ERK) (30). Activation of NF-κB and MAPKs in osteoclast precursors is believed to be involved in osteoclast differentiation. Recent studies (31) have revealed that TRAF6-mediated signals are particularly important for RANKL-induced osteoclast differentiation and function. TRAF6 knock-out mice exhibit severe osteopetrosis with defects in bone resorption due to the impaired osteoclast differentiation and function (32, 33). In contrast to RANK, TNF receptors interact with TRAF2 but not with TRAF6 in their signaling pathway (34).

Transforming growth factor β (TGF-β)-activated kinase 1 (TAK1) was first identified as a MAPK kinase kinase (MAPKKK) activated by TGF-β family ligands (35). Recent studies (36–38) have shown that TAK1, which forms a complex with the TAK1-binding protein 1 and 2 (TAB1/2), functions as an adaptor molecule in the interaction between TRAF6 and downstream molecules such as NF-κB, JNK, and p38 MAPK in signaling cascades induced by IL-1, LPS, and RANKL. Endogenous TAK1 is activated in response to RANKL stimulation, and a dominant-negative form of TAK1 inhibits the RANK-induced activation of NF-κB in RAW264.7 cells (38). It has been shown that TAK1 is also involved in TRAF2-mediated signaling (39). These results suggest that TAK1 is involved in the RANK- and TNF-receptor-induced signaling pathways and may regulate the MAPK and NF-κB pathways activated by the interaction of RANKL-RANK or TNFα-TNF receptors. AQ: B

In the present study, we explored the mechanism of PGE_2 action on the osteoclastic differentiation of precursor cells. The stimulatory effect of PGE_2 on the RANKL-induced osteoclast differentiation of the precursor cells was mediated through EP2 and EP4. TAK1 acted as an adaptor molecule linking PKA-induced signals, and RANKL and TNFα induced such signals in osteoclast precursors. Furthermore, TAK1 is involved in the synergistic effect of cAMP/PKA signals on TNF receptor- and Toll-like receptor 4 (TLR4)-induced signaling pathways. The cAMP/PKA signal may enhance bone resorption induced by RANKL and TNFα through TAK1 in osteoclast precursors.

EXPERIMENTAL PROCEDURES

Antibodies and Chemicals—Human recombinant RANKL was purchased from PeproTech EC Ltd. (London, UK), and mouse TNFα was from R & D Systems (Minneapolis, MN). Human M-CSF (Leukoprol) was obtained from Kyowa Hakko Kogyo Co. (Tokyo, Japan). PGE_2 were purchased from Wako Pure Chemical Industries Ltd. (Osaka, Japan). Purified LPS (*Escherichia coli* 055:B5) was from Sigma. Elcatonin, a synthetic analogue of eel calcitonin (CT), was kindly provided by Asahi Kasei (Tokyo, Japan). Forskolin and 3-isobutyl-1-methylxanthine (IBMX) were from Biomol (Plymouth Meeting, PA). Polyclonal antibodies against p38 MAPK, phosphorylated p38 MAPK, ERK, phosphorylated ERK, JNK, phosphorylated JNK, phospho-(Ser/Thr) PKA substrates, and IκBα were purchased from Cell Signaling Technology Inc. (Beverly, MA). Mouse monoclonal antibody against TAK1 was from Santa Cruz Biotechnology (Santa Cruz, CA). Fluo-4 AM, Fura Red AM, and Pluronic F127 were from Molecular Probes Inc. (Eugene OR). All other chemicals were of analytical grade.

Plasmids and cDNA Cloning—Mouse TAK1 cDNA (GenBank™ accession number D76446) was amplified by RT-PCR from cDNA of RAW264.7 cells using high fidelity Taq polymerase (Pyrobest, Takara Biochemicals, Tokyo, Japan) and TAK1-specific primers (forward primer 5′-gATATCCTGTCGACAGCCTCCGC and reverse primer 5′-AACGTAACGGGCCCAGAGAA). The PCR product was verified to be TAK1 cDNA by DNA sequencing. The TAK1 cDNA fragment was inserted into the BamHI-EcoRI site of pc DNA3.1/His, a mammalian expression vector (Invitrogen). The mutant TAK1, $Ser^{412} \rightarrow$ Ala TAK1, was generated by PCR-directed site-specific mutagenesis. Coding regions of all plasmids were sequenced in both directions prior to the transfection. AQ: C

Cell Culture and Transfection—RAW264.7 cells were obtained from RIKEN Cell Bank (Tsukuba, Japan) (RCB0535). RAW 264.7 cells were maintained in RPMI 1640 medium (Invitrogen) supplemented with 10% FBS (JRH Biosciences, Lenexa, KS) in 100-mm dishes. The RAW264.7 cells were transfected with the indicated expression plasmids (10 μg) by TransFast transfection reagents (Promega Corp., Madison, WI) according to the manufacturer's instructions. After 24 h of cultivation, 1 mg/ml of G418 was added to the medium, and the medium was replaced 2–3 times during a 2-week period. Clonal lines were prepared from the drug-resistant cultures. To evaluate clones expressing the TAK1 transgenes, Western blotting was performed on several cell lines. We obtained three different lines in each transfectant.

Cultures of Bone Marrow-derived Macrophages and RAW264.7 Cells—Bone marrow-derived macrophages (BMMϕ) were prepared as osteoclast precursors from 5- to 8-week-old male ddY mice (Shizuoka Laboratories Animal Center, Shizuoka, Japan). All procedures for animal care were approved by the Animal Management Committee of Matsumoto Dental University. Bone marrow cells obtained from mouse tibia were suspended in α-MEM (Sigma) supplemented with 10% FBS in 60-mm diameter dishes for 16 h in the presence of M-CSF (50 ng/ml). Then nonadherent cells were harvested and further cultured for 2 days with M-CSF (50 ng/ml). The adherent cells, most of which expressed macrophage-specific antigens such as Mac-1, Moma-2, and F4/80, were used as BMMϕ. RAW264.7 cells were cultured in α-MEM in the presence of RANKL (50 ng/ml) to induce their differentiation into osteoclasts. After the cells were cultured for 5 days, they were fixed and stained for tartrate-resistant acid phosphatase (TRAP, a marker enzyme of osteoclasts). TRAP-positive multinucleated cells containing more than three nuclei were observed under a microscope and counted as osteoclasts. The results were expressed as the mean ± S.D. of quadruplicate cultures. All experiments were performed at least three times, and similar results were obtained. Statistical analysis of the results was performed by Student's *t* test.

RT-PCR for PGE_2 Receptor mRNAs—Total RNA was extracted from cultured mouse bone marrow macrophages and RAW264.7 cells using the acid guanidinium-phenol-chloroform method. cDNA was synthesized from 10 μg of the total RNA by using reverse transcriptase (Revatra Ace, Toyobo Co. Ltd., Tokyo) and amplified using PCR. Sequences of primers used in RT-PCR for EP subtypes, CT receptor, and mouse glyceraldehyde-3-phosphate dehydrogenase (G3PDH) were described in previous reports (21, 40). The PCR conditions for EP subtypes were as follows: denaturation 94 °C, 30 s, annealing 65 °C, 30 s, and primer extension 75 °C, 60 s. The conditions for the CT receptor and G3PDH were as follows: denaturation 94 °C, 30 s, annealing 60 °C, 30 s, and primer extension 72 °C, 60 s. Preliminary experiments were performed to ensure that the number of PCR cycles was within the exponential phase of the amplification curve. PCR products were subjected to electrophoresis in a 2% agarose gel followed by staining with ethidium bromide. AQ: D

Immunoprecipitation and Western Blotting—Cells were washed once with phosphate-buffered saline and lysed in 200 μl of 0.1% Nonidet P-40 lysis buffer (20 mM Tris (pH 7.5), 50 mM β-glycerophosphate, 150 mM NaCl, 1 mM EDTA, 25 mM NaF, 1 mM sodium orthovanadate, 1× protease inhibitors mixture (Sigma)). After removal of the cellular debris, the lysates (1 mg of protein) were incubated with 1 μg of various antibodies and 20 μl of protein G-Sepharose (Amersham Biosciences). The immune complexes were washed three times with Nonidet P-40 lysis buffer. The Sepharose beads were suspended in 30 μl of Laemmli sample buffer and boiled for 2 min. The cell lysates and immunoprecipitates were resolved by SDS-PAGE and transferred onto a nitrocellulose membrane (Clear blot P membrane, Atto Instruments, Tokyo, Japan). The membrane was blotted with antibodies to specific proteins and visualized using the enhanced chemiluminescence system (Amersham Biosciences).

Assay of cAMP Production and IL-6—To measure the amount of cAMP produced, cells were preincubated for 5 min at 37 °C in α-MEM

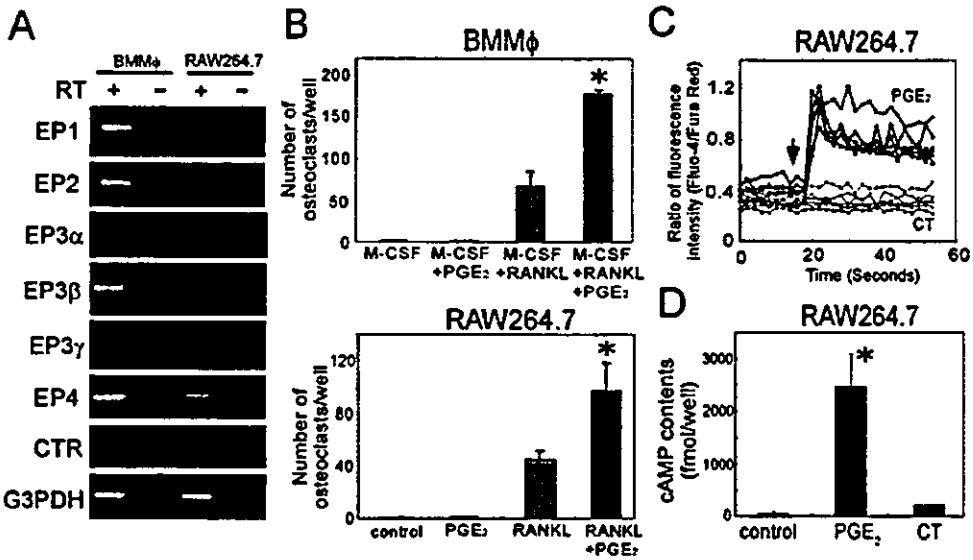

FIG. 1. **Expression of EP subtypes in mouse bone marrow macrophages and RAW264.7 cells.** *A*, RT-PCR analysis of EP subtypes in mouse bone marrow macrophages and RAW264.7 cells. Total RNA was extracted from mouse BMMϕ and RAW264.7 cells, and cDNA was synthesized from the total RNA by using reverse transcriptase. The expression of mRNA of EP1, EP2, EP3α, EP3β, EP3γ, EP4, CT receptor (*CTR*), and G3PDH was detected by PCR in the presence (+) or absence (−) of RT. *B*, effects of PGE_2 on osteoclast differentiation induced by RANKL. BMMϕ cells were cultured with or without PGE_2 (10^{-6} M) or RANKL (50 ng/ml) or RANKL plus PGE_2 in the presence of M-CSF (50 ng/ml) (*upper panel*). RAW264.7 cells were cultured with or without PGE_2 (10^{-6} M), RANKL (50 ng/ml), or RANKL plus PGE_2 (*lower panel*). After the cells were cultured for 5 days, they were fixed and stained for TRAP, and TRAP-positive multinucleated cells containing more than three nuclei were counted as osteoclasts. Results are expressed as the mean ± S.D. of quadruplicate cultures. *, significantly different between the culture treated with RANKL + M-CSF and that treated with RANKL + M-CSF + PGE_2 (*upper panel*), or between that with RANKL and that with RANKL + PGE_2 (*lower panel*); $p < 0.01$. *C*, effects of PGE_2 and CT on calcium signaling in RAW264.7 cells. RAW264.7 cells loaded with fluo-4 AM, Fura Red AM, and Pluronic F127 were subjected to calcium measurement. Cells were excited at 488 nm, and emission at 505–530 nm for fluo-4 and at 600–680 nm for Fura Red was acquired simultaneously at 2-s intervals. Cells were stimulated by the addition (an *arrow*) of PGE_2 (10^{-5} M) or CT (10^{-9} M). The ratio of the fluorescence intensity of fluo-4 to Fura Red was calculated to estimate intracellular Ca^{2+} influx in single cells. The results represent calcium signals in six single cells treated with PGE_2 or CT. *D*, effects of PGE_2 and CT on cAMP production in RAW264.7 cells. RAW264.7 cells were preincubated for 5 min with IBMX (1 mM) and then incubated for 5 min with PGE_2 (10^{-6} M) or CT (10^{-9} M). The amounts of intracellular cAMP were determined by ELISA. *, significantly different from the control culture; $p < 0.01$.

containing 1 mM IBMX, and then incubated for 5 min at 37 °C with CT (Elcatonin, 10^{-9} M) or PGE_2 (10^{-6} M). Cells were washed with ice-cold phosphate-buffered saline containing 1 mM IBMX and then were dissolved. The amounts of intracellular cAMP were determined using a cAMP enzyme immunoassay kit (Amersham Biosciences). To determine the effect of forskolin on LPS-induced IL-6 production, RAW264.7 cells transfected with mock, wild-type TAK1, or $Ser^{412} \rightarrow$ Ala TAK1 (0.8×10^5 cells/well, 48-well plate) were cultured with or without LPS (100 ng/ml) in the presence or absence of forskolin (100 μM) for 24 h. The culture medium was collected, and the concentration of IL-6 in the culture medium was measured by ELISA (R & D Systems).

Measurements of Intracellular Ca^{2+}—The effects of PGE_2 and CT on intracellular Ca^{2+} in RAW264.7 cells was measured using a confocal microscope (LSM510, Carl Zeiss, Jena, Germany) according to the methods described previously (41). RAW264.7 cells were incubated in glass-bottom dishes (Asahi Techno Glass Corp., Tokyo) for 6 h. Cells were then incubated with 5 μM fluo-4 AM, 5 μM Fura Red AM, and 0.05% Pluronic F127 for 30 min in Dulbecco's modified Eagle's medium. Cells loaded with these dyes were washed twice with α-MEM and post-incubated in α-MEM containing 10% FBS. Cells were further washed three times with Hanks' balanced salt solution and then excited at 488 nm. Emission at 505–530 nm for fluo-4 and at 600–680 nm for Fura Red was acquired simultaneously at 2-s intervals. The ratio of the fluorescence intensity of fluo-4 to Fura Red was calculated to estimate intracellular Ca^{2+} influx in single cells.

RESULTS

Expression of PGE_2 Receptors in Osteoclast Precursors—We first analyzed the expression of PGE_2 receptors in bone marrow macrophages and RAW264.7 cells using RT-PCR. Bone marrow macrophages expressed EP1, EP2, EP3β, and EP4 mRNAs, whereas RAW264.7 cells expressed EP1, EP2, and EP4 mRNAs (Fig. 1*A*). Bone marrow macrophages differentiated into TRAP-positive osteoclasts in response to RANKL together with M-CSF (Fig. 1*B*, *upper panel*). PGE_2 (10^{-6} M) alone did not induce osteoclast formation in cultures of bone marrow macrophages but did enhance the osteoclast formation induced by RANKL plus M-CSF (Fig. 1*B*, *upper panel*). RAW264.7 cells differentiated into osteoclasts in the presence of RANKL (Fig. 1*B*, *lower panel*). PGE_2 similarly enhanced the osteoclast differentiation induced by RANKL in cultures of RAW264.7 cells (Fig. 1*B*, *lower panel*). EP1 activates Ca^{2+} signals, whereas EP2 and EP4 couple to G_s protein, which stimulates adenylate cyclase activity. We then examined calcium signaling in RAW264.7 cells treated with PGE_2 and eel CT (Fig. 1*C*). An increase in intracellular calcium was induced by PGE_2 (10^{-5} M) but not CT (10^{-9} M) in RAW264.7 cells. We next examined the effects of PGE_2 and CT on cAMP production in RAW264.7 cells (Fig. 1*D*). PGE_2 (10^{-6} M) but not CT (10^{-9} M) stimulated cAMP production in RAW264.7 cells. We also analyzed the expression of EPs in osteoclasts purified from co-cultures of mouse calvarial osteoblasts and bone marrow cells treated with 1α,25-dihydroxyvitamin D_3. Osteoclasts expressed only EP1 mRNA but not EP2, EP3, or EP4 mRNA (data not shown). These results indicate that expression of EP2 and EP4 mRNAs in osteoclast precursors was down-regulated during their differentiation into osteoclasts. CT (10^{-9} M) enhanced intracellular calcium concentrations and cAMP production in osteoclasts formed from RAW264.7 cells treated with RANKL (data not shown). These results suggest that functional EP1, EP2, and EP4 are expressed in RAW264.7 cells.

Enhancement of RANKL-induced Osteoclast Differentiation by EP2/EP4-mediated Signals—PGE_2 has been shown to enhance synergistically RANKL-induced osteoclast differentiation from the precursors (26, 27). RAW264.7 cells expressed functional EP1, EP2, and EP4 receptors (Fig. 1). We then

F1

AQ: L

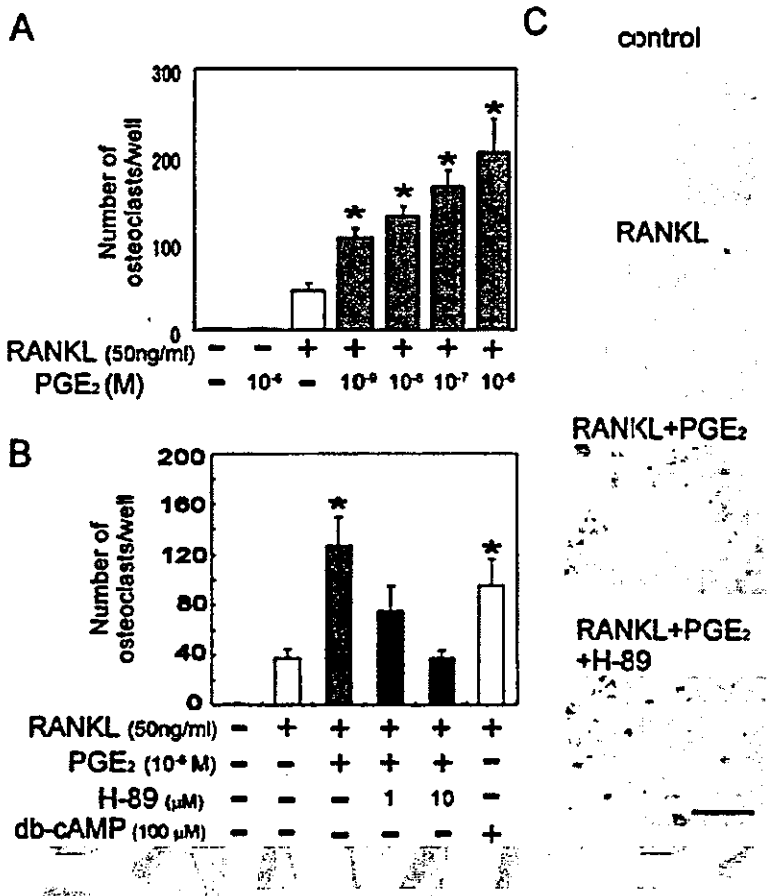

FIG. 2. **Enhancement of RANKL-induced osteoclast differentiation by EP2/EP4-mediated signals in RAW264.7 cells.** *A*, dose-dependent effects of PGE_2 on RANKL-induced osteoclast formation in RAW 264.7 cells. RAW264.7 cells were cultured with or without various concentrations of PGE_2 in the presence or absence of RANKL (50 ng/ml). After the cells were cultured for 5 days, they were fixed and stained for TRAP, and TRAP-positive multinucleated cells containing more than three nuclei were counted as osteoclasts. Results are expressed as the mean ± S.D. of quadruplicate cultures. *, significantly different between the culture treated with RANKL and that with RANKL + PGE_2; $p < 0.01$. *B*, effects of PGE_2, H-89, and Bt_2cAMP (*db-cAMP*) on RANKL-induced osteoclast formation in RAW264.7 cell cultures. RAW264.7 cells were cultured with or without RANKL (50 ng/ml), PGE_2 (10^{-6} M), H-89 (1 μM, 10 μM), and/or Bt_2cAMP (100 μM). After the cells were cultured for 5 days, they were fixed and stained for TRAP, and TRAP-positive multinucleated cells were counted as osteoclasts. Results are expressed as the mean ± S.D. of quadruplicate cultures. *, significantly different between the culture treated with RANKL and that with RANKL together with H89 or Bt_2cAMP; $p < 0.01$. *C*, TRAP staining of RAW264.7 cells treated with or without RANKL, RANKL + PGE_2, or RANKL + PGE_2 + H-89 (10 μM). *Bar* = 25 μm.

examined which type of PGE_2 receptors is involved in the stimulatory effect of PGE_2 on osteoclastic differentiation of RAW264.7 cells (Fig. 2). RANKL-induced osteoclast formation was enhanced by PGE_2 in a dose-dependent manner (Fig. 2*A*). The synergistic effect of PGE_2 on RANKL-induced osteoclast differentiation was dose-dependently inhibited by H-89, a specific inhibitor of PKA (Fig. 2, *B* and *C*). Dibutyryl cAMP (100 μM), a cell-permeable analogue of cAMP, enhanced the osteoclast differentiation induced by RANKL (Fig. 2*B*). PGE_2 and dibutyryl cAMP also enhanced osteoclastic differentiation of bone marrow macrophages treated with M-CSF and RANKL (data not shown). These results suggest that PGE_2 enhances RANKL-induced osteoclast differentiation through the signals mediated by EP2 and EP4 in the precursor cells.

Enhancement of RANK-induced Signals by EP2/EP4-mediated Signals—Binding of RANKL to RANK activates various signaling pathways, including those involving NF-κB, p38 MAPK, ERK, and JNK, in the target cells. We and others (42, 43) have demonstrated previously that p38 MAPK activity is essentially involved in RANKL-induced osteoclastic differentiation. We first examined the effects PGE_2 (10^{-6} M) on the phosphorylation of p38 MAPK in RAW264.7 cells in the presence or absence of RANKL (50 ng/ml) (Fig. 3*A*). PGE_2 alone failed to induce the phosphorylation of p38 MAPK in RAW264.7 cells but synergistically enhanced RANKL-induced phosphorylation of p38 MAPK within 15 min. Pretreatment of RAW264.7 cells with H-89 (10 μM) completely inhibited the synergistic effect of PGE_2 on RANKL-induced phosphorylation of p38 MAPK (Fig. 3*B*). This suggests that the stimulatory effect of PGE_2 on RANKL-induced phosphorylation of p38 MAPK is mediated by PKA. We then examined the effects of PGE_2 on the activation of NF-κB, p38 MAPK, ERK, and JNK in RAW264.7 cells treated with RANKL at different time points

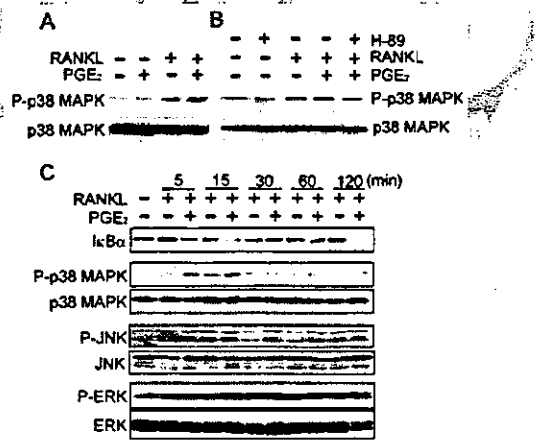

FIG. 3. **Effects of PGE_2 on RANKL-induced activation of MAPKs and NF-κB in RAW264.7 cells.** *A*, effects of PGE_2 on RANKL-induced phosphorylation of p38 MAPK in RAW264.7 cells. RAW264.7 cells were incubated for 15 min with or without PGE_2 (10^{-6} M), RANKL (50 ng/ml), or RANKL plus PGE_2. Cell lysates were prepared, immunoblotted with anti-phosphorylated-p38 MAPK antibody (*P-p38 MAPK*), and re-blotted with anti-p38 MAPK antibody (*p38 MAPK*). *B*, effect of H-89 on PGE_2-induced enhancement of phosphorylation of p38 MAPK in RAW264.7 cells. RAW264.7 cells were pre-cultured for 1 h in the presence or absence of H-89 (10 μM) and then incubated for 15 min with or without RANKL (50 ng/ml) in the presence or absence of PGE_2 (10^{-6} M). Cell lysates were prepared, immunoblotted with anti-phosphorylated p38 MAPK antibody, and re-blotted with anti-p38 MAPK antibody. *C*, time course of changes in degradation of IκBα and phosphorylation of p38 MAPK, JNK, and ERK in RAW264.7 cells. RAW264.7 cells were incubated with RANKL (50 ng/ml) in the presence or absence of PGE_2 (10^{-6} M) for the indicated times. Cell lysates were prepared and immunoblotted with the antibodies indicated in the panel. Amounts of p38 MAPK, JNK, and ERK in the lysates were determined by re-blotting the membrane with the indicated antibodies.

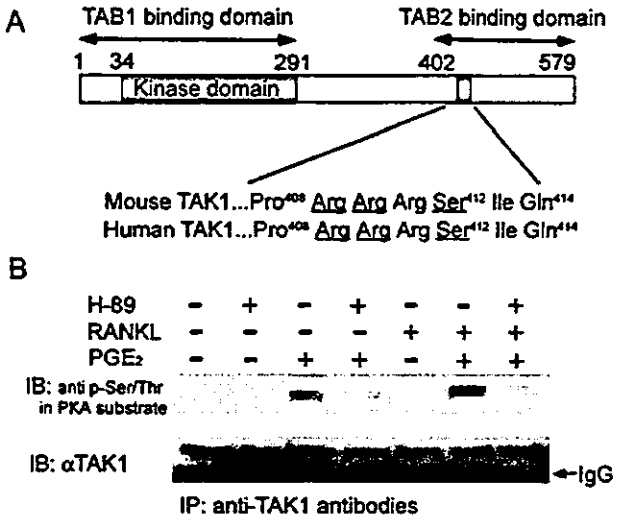

FIG. 4. **Effects of PGE_2 and H-89 on phosphorylation of TAK1 in RAW264.7 cells.** *A*, structure of TAK1. TAK1 possesses the kinase domain in the N-terminal region, the TAB1-binding domain in the kinase domain, and the TAB2-binding domain in the C-terminal region. A consensus motif (RRXS motif) recognized by PKA is located in the C-terminal region and consists of Arg^{408}-Arg-Arg-Ser-Ilu-Gln^{414} in mouse and human TAK1. *B*, phosphorylation of TAK1 in RAW264.7 cells treated with PGE_2. RAW264.7 cells were pre-cultured for 1 h in the presence or absence of H-89 (10 μM) and then stimulated with or without RANKL (50 ng/ml) in the presence or absence of PGE_2 (10^{-6} M) for 15 min. Cell lysates were subjected to immunoprecipitation with anti-TAK1 antibody. The immunoprecipitates were separated, immunoblotted (*IB*) with antibody against phosphorylated Ser/Thr in PKA substrates, and re-blotted with anti-TAK1 antibody.

(Fig. 3*C*). PGE_2 synergistically enhanced RANKL-induced degradation of IκBα (NF-κB activation) and phosphorylation of p38 MAPK in RAW264.7 cells for 5–15 min. RANKL-induced phosphorylation of JNK was also enhanced by PGE_2 for 15–30 min (Fig. 3*C*). The synergistic effect of PGE_2 on RANKL-induced phosphorylation of ERK was much weaker than on RANKL-induced phosphorylation of p38 MAPK in RAW264.7 cells throughout the experimental period. These results suggest that PKA-induced signals mainly cross-talk with an upstream effector(s) of p38 MAPK, NF-κB, and JNK.

Involvement of TAK1 in EP2/EP4-mediated Enhancement of RANKL-induced Signals and Osteoclast Differentiation—PKA recognizes a consensus sequence (RRX(S/T) motif) of the target proteins and phosphorylates the Ser/Thr residue in the sequence (44, 45). We searched for effectors having the RRX(S/T) motif in RANK-induced signaling molecules, including TRAF6, TAK1, TAB1, TAB2, and other MAPKKs and MAPKKKs. We found that murine TAK1 contains a consensus PKA recognition sequence (Arg^{408}-Arg-Arg-Ser-Ilu-Gln^{414}) at the C-terminal region (Fig. 4*A*). Human TAK1 also possesses this consensus motif. Recent studies showed that in IL-1 and RANKL-induced signaling cascades, TAK1 functioned as an adaptor molecule in the interaction between TRAF6 and the downstream molecules such as NF-κB and MAPKs (36, 38). We then examined whether the endogenous TAK1 was phosphorylated in RAW264.7 cells in response to PGE_2 (10^{-6} M) (Fig. 4*B*). Phosphorylation of TAK1 detected by antibody against phosphorylated Ser/Thr of PKA substrates was markedly induced in RAW264.7 cells treated with PGE_2 (Fig. 4*B*). The phosphorylation of TAK1 induced by PGE_2 was strongly suppressed by pretreatment of RAW264.7 cells with H-89 (10 μM). RANKL (50 ng/ml) failed to induce phosphorylation of Ser/Thr residues in TAK1 and showed no effect on the PGE_2-induced phosphorylation of TAK1. These results suggest that PGE_2-induced phosphorylation of TAK1 is PKA-dependent in RAW264.7 cells.

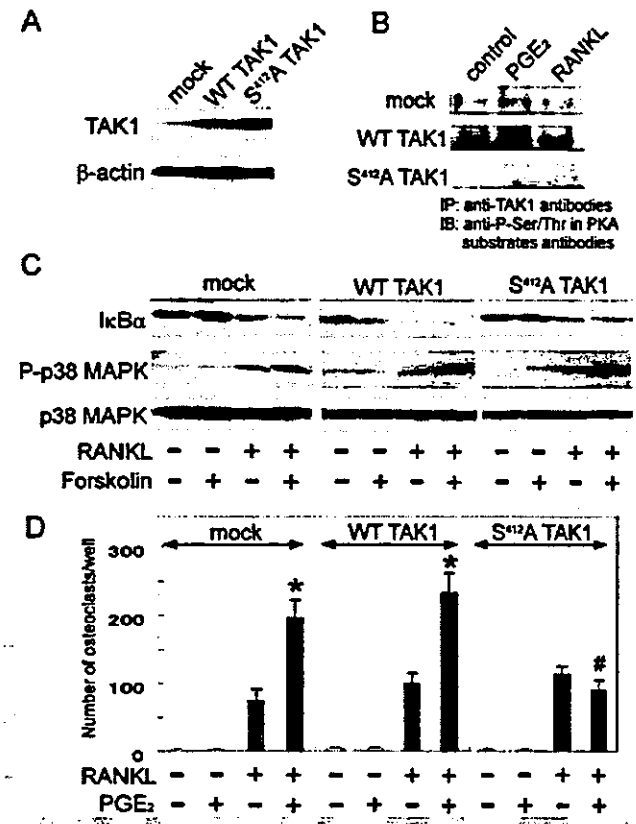

FIG. 5. **Effect of Ser^{412} → Ala TAK1 on PGE_2-induced up-regulation of osteoclast differentiation in RAW264.7 cells treated with RANKL.** *A*, transfection of RAW264.7 cells with wild-type TAK1 or Ser^{412} → Ala ($S^{412}A$) TAK1 cDNAs. RAW264.7 cells were stably transfected with mock, wild-type TAK1 (*WT TAK1*), or S412A TAK1. Cell lysates were prepared, immunoblotted with anti-TAK1 antibody, and re-blotted with anti-β-actin antibody. *B*, phosphorylation of TAK1 in RAW264.7 cells transfected with mock, WT TAK1, and S412A TAK1. RAW264.7 cells stably expressing mock, WT TAK1, or S412A TAK1 were treated with or without PGE_2 (10^{-6} M) or RANKL (50 ng/ml) for 15 min. Cell lysates were subjected to immunoprecipitation with anti-TAK1 antibody. The immunoprecipitates (*IP*) were separated and immunoblotted (*IB*) with antibodies against phosphorylated Ser/Thr in PKA substrates. *C*, effects of forskolin on the activation of NF-κB and p38 MAPK induced by RANKL in RAW264.7 cells transfected with mock, WT TAK1, and S412A TAK1. RAW264.7 cells transfected with mock, WT TAK1, or S412A TAK1 were treated with or without RANKL (50 ng/ml) in the presence or absence of forskolin (100 μM) for 15 min. Cell lysates were separated and immunoblotted with anti-IκBα antibody (*IκBα*) and with anti-phosphorylated-p38 MAPK antibody (*P-p38 MAPK*) followed by re-blotting with anti-p38 MAPK antibody (*p38 MAPK*). *D*, effect of PGE_2 on RANKL-induced osteoclast formation in RAW264.7 cells transfected with mock, WT TAK1, and S412A TAK1. RAW264.7 cells transfected with mock, WT TAK1, or S412A TAK1 were cultured with or without RANKL (50 ng/ml) in the presence or absence of PGE_2 (10^{-6} M). After the cells were cultured for 5 days, cells were fixed and stained for TRAP. TRAP-positive multinuclear cells containing three or more nuclei were counted as osteoclasts. Results are expressed as the mean ± S.D. of quadruplicate cultures. *, significantly different between cultures treated with RANKL and those with RANKL + PGE_2 in each cDNA transfectant; $p < 0.01$. #, significantly different between mock-transfected cultures and wild-type TAK1- or Ser^{412} → Ala TAK1-transfected cultures in the same treatment groups; $p < 0.01$.

We further analyzed whether the Ser^{412} residue in TAK1 was phosphorylated in RAW264.7 cells in response to PGE_2 by using a Ser^{412} → Ala mutant form of TAK1 (Ser^{412} → Ala TAK1). RAW264.7 cells were stably transfected with empty vector (mock) or expression vector for wild-type TAK1 or Ser^{412} → Ala TAK1 (Fig. 5*A*). Endogenous and transfected wild-type TAK1 were phosphorylated in response to PGE_2 (10^{-6} M) but not to RANKL (50 ng/ml) in RAW264.7 cells (Fig. 5*B*). In

contrast, when RAW264.7 cells were transfected with $Ser^{412} \rightarrow$ Ala TAK1, the phosphorylation of both endogenous and transfected TAK1 was strongly suppressed even in the presence of PGE_2 (Fig. 5*B*). The other two RAW264.7 cell lines established using each transfectant showed similar responsiveness to RANKL and PGE_2 (data not shown). This suggests that $Ser^{412} \rightarrow$ Ala TAK1 acts as a dominant-negative mutant in RAW264.7 cells. We then examined whether PKA-induced phosphorylation of TAK1 was involved in the synergistic effect on the RANK-induced signals (Fig. 5*C*). RANKL-induced degradation of IκBα and phosphorylation of p38 MAPK were enhanced by forskolin (100 μM), an activator of PKA, in RAW264.7 cells transfected with mock or wild-type TAK1 but not in those transfected with $Ser^{412} \rightarrow$ Ala TAK1 (Fig. 5*C*). RAW264.7 cells transfected with mock or wild-type TAK1 differentiated into osteoclasts in response to RANKL (50 ng/ml), and PGE_2 (10^{-6} M) enhanced RANKL-induced osteoclast differentiation (Fig. 5*D*). RANKL similarly stimulated osteoclastic differentiation of RAW264.7 cells transfected with $Ser^{412} \rightarrow$ Ala TAK1. However, the stimulatory effect of PGE_2 on RANKL-induced osteoclast differentiation was suppressed in RAW264.7 cells expressing $Ser^{412} \rightarrow$ Ala TAK1. These results suggest that EP2/EP4 signals induce the phosphorylation of TAK1 in osteoclast precursors, which in turn enhances RANK-mediated signals that induce osteoclast differentiation.

Involvement of TAK1 in PKA-mediated Enhancement of TNFα-induced Signals and Osteoclast Differentiation—We and others (13–15) have also reported that TNFα stimulated osteoclastic differentiation from osteoclast precursors through a mechanism independent of the RANKL-RANK interaction. TAK1 is also implicated in the TNF receptor-mediated signaling (39). We then examined whether PKA-mediated signals enhanced TNFα-induced osteoclast differentiation through TAK1-mediated signals (Fig. 6). TNFα (40 ng/ml) stimulated degradation of IκBα and phosphorylation of p38 MAPK in RAW264.7 cells transfected with mock or wild-type TAK1, both of which were enhanced by forskolin (100 μM) (Fig. 6*A*). In contrast, the synergistic effects of forskolin on the degradation of IκBα and phosphorylation of p38 MAPK were completely suppressed by the transfection with $Ser^{412} \rightarrow$ Ala TAK1. TNFα (40 ng/ml) stimulated osteoclastic differentiation of RAW264.7 cells transfected with mock or wild-type TAK1, and forskolin (100 μM) enhanced TNFα-induced osteoclastic differentiation in those transfected cells (Fig. 6*B*). TNFα similarly stimulated osteoclastic differentiation of RAW264.7 cells transfected with $Ser^{412} \rightarrow$ Ala TAK1, but the stimulatory effect of forskolin on TNFα-induced osteoclast differentiation was completely suppressed in those cells (Fig. 6*B*). These results suggest that the phosphorylation of TAK1 by PKA signals synergistically enhances TNFα-induced activation of p38 MAPK and NF-κB and osteoclast differentiation in cultures of RAW264.7 cells.

F6

Involvement of TAK1 in PKA-mediated Enhancement of LPS-induced IL-6 Production—PGE_2 has been shown to enhance LPS-induced IL-6 mRNA expression in mouse macrophages (46). LPS activates NF-κB and MAPKs through TAK1 in TLR4 signaling (37). We finally examined whether the phosphorylation of Ser^{412} in TAK1 by PKA is involved in PGE_2-induced enhancement of IL-6 production (Fig. 7). LPS (100 ng/ml) stimulated degradation of IκBα and phosphorylation of p38 MAPK in RAW264.7 cells transfected with either mock, wild-type TAK1, or $Ser^{412} \rightarrow$ Ala TAK1. Forskolin (100 μM) enhanced LPS-induced degradation of IκBα and phosphorylation of p38 MAPK in RAW264.7 cells transfected with mock or wild-type TAK1 (Fig. 7*A*). The synergistic effects of forskolin on LPS-induced degradation of IκBα and phosphorylation of p38 MAPK were strongly suppressed in RAW264.7 cells transfected with $Ser^{412} \rightarrow$ Ala TAK1. Forskolin (100 μM) enhanced LPS-induced IL-6 production in RAW264.7 cells transfected with mock or wild-type TAK1 (Fig. 7*B*). The stimulatory effect of forskolin on the LPS-induced IL-6 production was significantly suppressed in RAW264.7 cells transfected with $Ser^{412} \rightarrow$ Ala TAK1.

F7, AQ: E

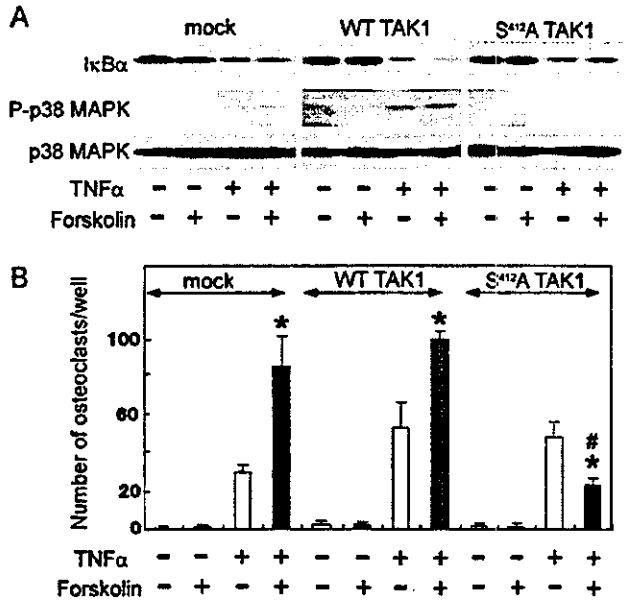

FIG. 6. **Effect of $Ser^{412} \rightarrow$ Ala TAK1 on forskolin-induced up-regulation of osteoclast differentiation in RAW264.7 cells treated with TNFα.** *A*, effects of forskolin on the activation of NF-κB and p38 MAPK induced by TNFα in RAW264.7 cells transfected with mock, WT TAK1, and S412A TAK1. RAW264.7 cells transfected with mock, WT TAK1, or S412A TAK1 were treated with or without TNFα (40 ng/ml) in the presence or absence of forskolin (100 μM) for 15 min. Cell lysates were immunoblotted with anti-IκBα antibody (*IκBα*) or with anti-phosphorylated-p38 MAPK (*P-p38 MAPK*) antibody followed by re-blotting with anti-p38 MAPK antibody (*p38 MAPK*). *B*, effect of forskolin on TNFα-induced osteoclast formation RAW264.7 cells transfected with mock, WT TAK1, and S412A TAK1. RAW264.7 cells transfected with mock, WT TAK1, or S412A TAK1 were cultured with or without TNFα (40 ng/ml) in the presence or absence of forskolin (100 μM). After the cells were cultured for 5 days, cells were fixed and stained for TRAP. TRAP-positive multinuclear cells containing three or more nuclei were counted as osteoclasts. Results are expressed as the mean ± S.D. of quadruplicate cultures. *, significantly different between cultures treated with TNFα and those with TNFα + forskolin in each cDNA transfectant; $p < 0.01$. #, significantly different between mock-transfected cultures and WT TAK1- or S412A TAK1-transfected cultures in the same treatment groups; $p < 0.01$.

DISCUSSION

Previous studies have shown that PGE_2 stimulates osteoclastic bone resorption through two different mechanisms as follows: the induction of RANKL expression in osteoblasts (21, 22), and the direct enhancement of RANKL-induced differentiation of the precursor cells into osteoclasts (27). In the present study, we examined the mechanism of the synergistic effect of PGE_2 on RANKL-induced osteoclastic differentiation. We have shown here that PGE_2 synergistically enhances osteoclastic differentiation of RAW264.7 cells through EP2 and EP4, and that TAK1 is a key molecule in cAMP/PKA-induced up-regulation of osteoclast differentiation stimulated by not only RANKL but also TNFα.

Osteoclast precursors of bone marrow macrophages and RAW264.7 cells expressed EP1 as well as EP2 and EP4 (Fig. 1). Treatment of RAW264.7 cells with PGE_2 but not CT increased Ca^{2+} influx, suggesting that osteoclast precursors express functional EP1. The synergistic effect of PGE_2 on RANKL-induced osteoclast differentiation was inhibited by H-89, a

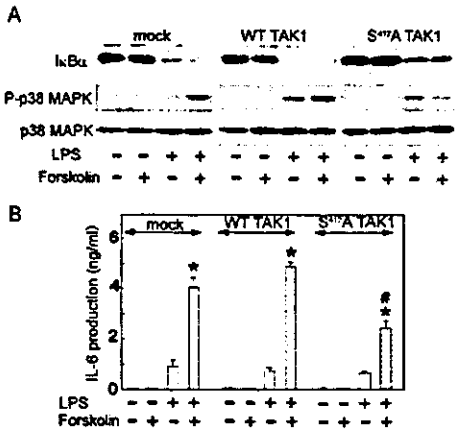

FIG. 7. **Effect of the Ser^{412} → Ala TAK1 on forskolin-induced up-regulation of IL-6 production in RAW264.7 cells treated with LPS.** *A*, effects of forskolin on the activation of NF-κB and p38 MAPK induced by LPS in RAW264.7 cells transfected with mock, WT TAK1, and S412A TAK1. RAW264.7 cells transfected with mock, WT TAK1, or S412A TAK1 were treated with or without LPS (100 ng/ml) in the presence or absence of forskolin (100 μM) for 15 min. Cell lysates were immunoblotted with anti-IκBα antibody (*IκBα*), or with anti-phosphorylated-p38 MAPK (*P-p38 MAPK*) antibody followed by re-blotting with anti-p38 MAPK antibody (*p38 MAPK*). *B*, effect of forskolin on LPS-induced IL-6 production in RAW264.7 cells transfected with mock, WT TAK1, and S412A TAK1. RAW264.7 cells transfected with mock, WT TAK1, or S412A TAK1 were cultured with or without LPS (100 ng/ml) in the presence or absence of forskolin (100 μM) for 24 h. The culture medium was then collected, and IL-6 concentrations were measured using an ELISA for IL-6. *, significantly different between cultures treated with LPS and those with LPS + forskolin in each transfectant; $p < 0.01$. Significantly different between mock-transfected cultures and WT TAK1- or S412A TAK1-transfected cultures in the same treatment groups; $p < 0.01$.

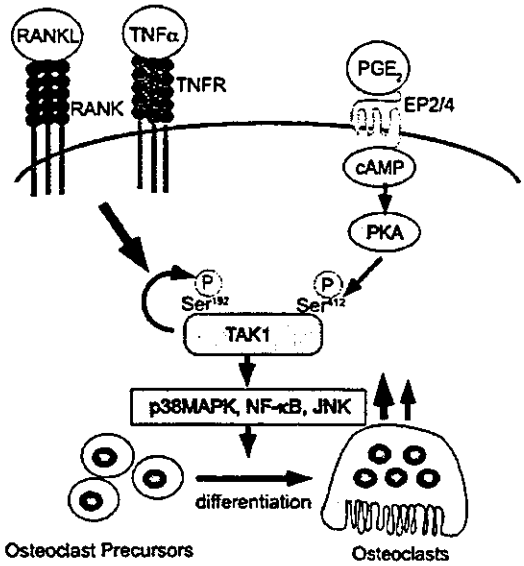

FIG. 8. **A possible role of phosphorylation of Ser^{412} in TAK1 in osteoclast differentiation induced by RANKL and TNFα.** Cyclic AMP-dependent PKA phosphorylates the Ser^{412} residue in TAK1 in osteoclast precursors in response to the binding of PGE2 to EP2 or EP4. The phosphorylation of TAK1 itself does not induce osteoclastic differentiation of the precursors but synergistically enhances downstream signals such as MAPKs and NF-κB in response to other factors including RANKL and TNFα. Phosphorylation of Ser^{192} in TAK1 appears to be indispensable for the signal transduction induced by RANKL and TNFα as well as IL-1 (47). Osteoclastic differentiation induced by RANKL and TNFα is also enhanced by the phosphorylation of the Ser^{412} residue of TAK1 in osteoclast precursors.

specific inhibitor of PKA, and dibutyryl cAMP enhanced the osteoclast differentiation induced by RANKL (Fig. 2). We further examined which receptor, EP2 or EP4, was mainly involved in the synergistic effect of PGE_2 on RANKL-induced osteoclastic differentiation of RAW264.7 cells, using specific EP1, EP2, and EP4 agonists. The number of osteoclasts formed in RAW264.7 cell cultures treated with 10^{-6} M ONO-AE1-259 (EP2 agonist) and 10^{-6} M ONO-AE1-329 (EP4 agonist) increased by 1.4 and 2.4 times, respectively (data not shown). In contrast, ONO-DI-004 (EP-1 agonist) at 10^{-6} M showed no effect on osteoclast formation in RAW264.7 cell cultures. Thus, the effect of EP agonists on osteoclast formation was comparable with the expression level of EP2 and EP4 mRNAs (Fig. 1A). These results suggest that EP4 mainly mediates the synergistic effect of PGE_2 on RANKL-induced osteoclast differentiation in RAW 264.7 cells.

TAK1 is a key MAPKKK in the IL-1 receptor- and TLR4-mediated signaling pathway (36, 37). TAK1 mediates MAPK and NF-κB activation via interaction with TRAF6, and TAB2 acts as an adaptor linking TAK1 and TRAF6. Mizukami *et al.* (38) first reported that TAK1 participates in the RANK signaling pathway. Endogenous TAK1 was activated in response to RANKL in RAW264.7 cells, and the kinase-negative form of TAK1 (K63W TAK1) attenuated JNK and NF-κB activation induced by RANKL. We have confirmed that expression of K63W TAK1 in RAW264.7 cells significantly inhibited the osteoclast formation induced by RANKL and TNFα.[2] By using antibody against phosphorylated Ser/Thr of PKA substrates, we showed that phosphorylated Ser/Thr of TAK1 was induced by PGE_2 (Figs. 4 and 5). However, the phosphorylated Ser/Thr of TAK1 was not detected in RAW264.7 cells transfected with the Ser^{412} → Ala mutant TAK1 (Fig. 5*B*), suggesting that Ser^{412} → Ala TAK1 acted as a dominant-negative mutant of TAK1. These findings indicate that Ser^{412} in TAK1 is a major phosphorylation site by PKA.

The expression of Ser^{412} → Ala TAK1 in RAW264.7 cells did not inhibit RANKL- or TNFα-induced osteoclast formation (Figs. 5 and 6). However, the expression of Ser^{412} → Ala TAK1 suppressed the PKA signal-mediated up-regulation of the degradation of IκBα degradation, phosphorylation of p38 MAPK, and osteoclast differentiation induced by RANKL and TNFα in RAW264.7 cells (Figs. 5 and 6). It was reported that Ser^{192} in the kinase domain in TAK1 was phosphorylated by the kinase in response to IL-1 stimulation, and the phosphorylation of Ser^{192} was important for the IL-1-induced signal transduction (47). These results together with our findings suggest that overexpression of wild-type or the Ser^{412} → Ala mutant TAK1 itself enhances osteoclastic differentiation induced by RANKL and TNF-α. The Ser^{412} residue appears to be involved in the synergistic action of cAMP/PKA signaling in osteoclast differentiation. Our experiments also suggest that the Ser^{412} residue regulates the synergistic action of cAMP/PKA signaling in osteoclast differentiation (Fig. 8).

TRAF6 plays essential roles in osteoclast differentiation and function induced by RANK-mediated signals (31–33). In contrast to RANK, TNF receptors selectively interact with TRAF2 in the signaling pathway (34). Forskolin enhanced TNFα-induced signals and osteoclast differentiation in cultures of RAW264.7 cells (Fig. 6). These results suggest that cAMP/PKA signals cross-talk with TRAF2-mediated signals as well as TRAF6-mediated ones. Recent studies (48) have shown that TAK1 is involved in not only TRAF6-mediated signaling but also TRAF2-mediated signaling. TNFα induced the binding of TAK1 to TRAF2 in HeLa cells. TAB2 has been shown to activate NF-κB by linking TAK1 to TRAF6 (49). Recently, it was

[2] Y. Kobayashi *et al.*, unpublished observations.

shown that TAB3, a TAB2-like molecule that associates with TAK1 and activates NF-κB, interacts with both TRAF2 and TRAF6 (39). RAW264.7 cells have been shown to express TAB3 as well as TAB2 (50). We have confirmed that those two molecules are expressed in bone marrow macrophages as well as RAW264.7 cells (data not shown). These results suggest that the interaction of TAK1 and TAB2 (or TAB3) is involved in osteoclast differentiation induced by RANKL and TNFα.

TLR and IL-1 receptors use myeloid differentiation factor 88 (MyD88) as a common signaling molecule (51). In response to LPS, MyD88 interacts with TRAF6, which activates downstream signals. Recent studies have shown that Toll-IL-1 receptor domain-containing adaptor inducing interferon-β (TRIF)-mediated signaling is involved in a MyD88-independent pathway induced by LPS (52). Both MyD88-dependent and TRIF-dependent pathways are required for LPS-induced cytokine production in macrophages (52). Forskolin significantly enhanced LPS-induced IκBα degradation, p38 MAPK phosphorylation, and IL-6 production in RAW264.7 cells (Fig. 7). In contrast to the effect of S412A TAK1 on PKA signal-enhanced osteoclast differentiation, the mutant TAK1 significantly but not completely suppressed forskolin-induced enhancement of IL-6 production in RAW264.7 cells treated with LPS. These results suggest that TAK1 signals are certainly involved in the PKA signal-induced enhancement of LPS signals, but signaling molecules other than TAK1 are also involved in the cross-talk between PKA-activated signals and TLR4-induced signals in macrophages. The TRIF-dependent pathway may be another target for the PKA signals in osteoclast precursors. McCoy *et al.* (53) reported that the production of IL-6 significantly decreased in EP4 receptor-deficient mice in collagen antibody-induced arthritis. Moreover, PKA signals have been shown to enhance LPS-induced IL-6 production in mouse macrophages and Swiss 3T3 cells (46, 54, 55). Thus, these previous findings and our study strongly support the idea that PKA-induced phosphorylation of TAK1 enhances LPS-induced IL-6 production, although we cannot completely rule out the possibility that there is an alternative target for PKA in TLR4 signaling.

AQ: G

At present, it is not known how the phosphorylation of TAK1 by PKA enhances TRAF6- and TRAF2-induced signals. However, it should be noted that the site phosphorylated by PKA is located in the TAB2 binding domain of the TAK1 molecule (Fig. 4). TAB3 has also been proposed to bind to the TAB2 binding domain (39). These results suggest that phosphorylation of TAK1 by PKA may influence the signaling complex formation (TAK1-TAB1-TAB2/TAB3) induced by the various ligands studied here. Therefore, we examined whether RANKL-induced formation of the complex of TAK1-TAB2 in RAW264.7 cells was affected by the treatment with PGE_2. However, we could not find significant changes in the complex formation in response to PGE_2 (data not shown). Further studies will be necessary to elucidate the molecular mechanism of the interaction between PKA-activated signals and TRAF-mediated signals in osteoclast precursors.

In conclusion, we demonstrated that PKA-activated signals enhanced RANKL-, TNFα-, and LPS-induced signals in osteoclast precursors. PKA selectively phosphorylated the Ser^{412} residue in TAK1, which was crucially involved in the synergistic action of PGE_2 on RANK-, TNF receptor-, and TLR-mediated signaling. The cAMP/PKA signal may enhance RANKL- and inflammatory cytokine-induced bone resorption through TAK1 in osteoclast precursors (Fig. 8). Signaling molecules involved in the TAK1 pathway in osteoclast precursors would be novel targets for drugs to inhibit osteoclast function induced by inflammatory diseases.

REFERENCES

1. Baron, R., Neff, L., Tran, V. P., Nefussi, J. R., and Vignery, A. (1986) *Am. J. Pathol.* **122**, 363–378
2. Ibbotson, K. J., Roodman, G. D., McManus, L. M., and Mundy, G. R. (1984) *J. Cell Biol.* **99**, 471–480
3. Osdoby, P., Martini, M. C., and Caplan, A. I. (1982) *J. Exp. Zool.* **224**, 331–344
4. Takahashi, N., Akatsu, T., Udagawa, N., Sasaki, T., Yamaguchi, A., Moseley, J. M., Martin, T. J., and Suda, T. (1988) *Endocrinology* **123**, 2600–2602
5. Suda, T., Takahashi, N., and Martin, T. J. (1992) *Endocr. Rev.* **13**, 66–80
6. Chambers, T. J. (2000) *J. Pathol.* **192**, 4–13
7. Suda, T., Takahashi, N., Udagawa, N., Jimi, E., Gillespie, M. T., and Martin, T. J. (1999) *Endocr. Rev.* **20**, 345–357
8. Teitelbaum, S. L., and Ross, F. P. (2003) *Nat. Rev. Genet.* **4**, 638–649
9. Suda, K., Udagawa, N., Sato, N., Takami, M., Itoh, K., Woo, J.-T., Takahashi, N., and Nagai, K. (2004) *J. Immunol.* **172**, 2504–2510
10. Lacey, D. L., Timms, E., Tan, H. L., Kelley, M. J., Dunstan, C. R., Burgess, T., Elliott, R., Colombero, A., Elliott, G., Scully, S., Hsu, H., Sullivan, J., Hawkins, N., Davy, E., Capparelli, C., Eli, A., Qian, Y. X., Kaufman, S., Sarosi, I., Shalhoub, V., Senaldi, G., Guo, J., Delaney, J., and Boyle, W. J. (1998) *Cell* **93**, 165–176
11. Yasuda, H., Shima, N., Nakagawa, N., Yamaguchi, K., Kinosaki, M., Mochizuki, S., Tomoyasu, A., Yano, K., Goto, M., Murakami, A., Tsuda, E., Morinaga, T., Higashio, K., Udagawa, N., Takahashi, N., and Suda, T. (1998) *Proc. Natl. Acad. Sci. U. S. A.* **95**, 3597–3602
12. Hsu, H., Lacey, D. L., Dunstan, C. R., Solovyev, I., Colombero, A., Timms, E., Tan, H.-L., Elliott, G., Kelley, M. J., Sarosi, I., Wang, L., Xia, X.-Z., Elliott, R., Chiu, L., Black, T., Scully, S., Capparelli, C., Morony, S., Shimamoto, G., Bass, M. B., and Boyle, W. J. (1999) *Proc. Natl. Acad. Sci. U. S. A.* **96**, 3540–3545
13. Kobayashi, K., Takahashi, N., Jimi, E., Udagawa, N., Takami, M., Kotake, S., Nakagawa, N., Kinosaki, M., Yamaguchi, K., Shima, N., Yasuda, H., Morinaga, T., Higashio, K., Martin, T. J., and Suda, T. (2000) *J. Exp. Med.* **191**, 275–286
14. Azuma, Y., Kaji, K., Katogi, R., Takeshita, S., and Kudo, A. (2000) *J. Biol. Chem.* **275**, 4858–4864
15. Lam, J., Takeshita, S., Barker, J. E., Kanagawa, O., Ross, F. P., and Teitelbaum, S. L. (2000) *J. Clin. Investig.* **106**, 1481–1488
16. Moreno, J. L., Kaczmarek, M., Keegan, A. D., and Tondravi, M. (2003) *Blood* **102**, 1078–1086
17. Sakuma, Y., Tanaka, K., Suda, M., Komatsu, Y., Yasoda, A., Miura, M., Ozasa, A., Narumiya, S., Sugimoto, Y., Ichikawa, A., Ushikubi, F., and Nakao, K. (2000) *Infect. Immun.* **68**, 6819–6825
18. Okada, Y., Lorenzo, J. A., Freeman, A. M., Tomita, M., Morham, S. G., Raisz, L. G., and Pilbeam, C. C. (2000) *J. Clin. Investig.* **105**, 823–832
19. Trebino, C. E., Stock, J. L., Gibbons, C. P., Naiman, B. M., Wachtmann, T. S., Umland, J. P., Pandher, K., Lapointe, J.-M., Saha, S., Roach, M. L., Carter, D., Thomas, N. A., Durtschi, B. A., McNeish, J. D., Hambor, J. E., Jakobsson, P.-J., Carty, T. J., Perez, J. R., and Audoly, L. P. (2003) *Proc. Natl. Acad. Sci. U. S. A.* **100**, 9044–9049
20. Miyaura, C., Inada, M., Matsumoto, C., Ohshiba, T., Uozumi, N., Shimizu, T., and Ito, A. (2003) *J. Exp. Med.* **197**, 1303–1310
21. Suzawa, T., Miyaura, C., Inada, M., Maruyama, T., Sugimoto, Y., Ushikubi, F., Ichikawa, A., Narumiya, S., and Suda, T. (2000) *Endocrinology* **141**, 1554–1559
22. Li, X., Okada, Y., Pilbeam, C. C., Lorenzo, J. A., Kennedy, C. R. J., Breyer, R. M., and Raisz, L. G. (2000) *Endocrinology* **141**, 2054–2061
23. Narumiya, S., and FitzGerald, G. A. (2001) *J. Clin. Investig.* **108**, 25–30
24. Narumiya, S., Sugimoto, Y., and Ushikubi, F. (1999) *Physiol. Rev.* **79**, 1193–1226
25. Tomita, M., Li, X., Okada, Y., Woodiel, F. N., Young, R. N., Pilbeam, C. C., and Raisz, L. G. (2002) *Bone (NY)* **30**, 159–163
26. Tintut, Y., Parhami, F., Tsingotjidou, A., Tetradis, S., Territo, M., and Demer, L. L. (2002) *J. Biol. Chem.* **277**, 14221–14226
27. Wani, M. R., Fuller, K., Kim, N. S., Choi, Y., and Chambers, T. (1999) *Endocrinology* **140**, 1927–1935
28. Darnay, B. G., Haridas, V., Ni, J., Moore, P. A., and Aggarwal, B. B. (1998) *J. Biol. Chem.* **273**, 20551–20555
29. Wong, B. R., Josien, R., Lee, S. Y., Vologodskaia, M., Steinman, R. M., and Choi, Y. (1998) *J. Biol. Chem.* **273**, 28355–28359
30. Boyle, W. J., Simonet, W. S., and Lacey, D. L. (2003) *Nature* **423**, 337–342
31. Kobayashi, N., Kadono, Y., Naito, A., Matsumoto, K., Yamamoto, T., Tanaka, S., and Inoue, J. (2001) *EMBO J.* **20**, 1271–1280
32. Lomaga, M. A., Yeh, W.-C., Sarosi, I., Duncan, G. S., Furlonger, C., Ho, A., Morony, S., Capparelli, C., Van, G., Kaufman, S., van der Heiden, A., Itie, A., Wakeham, A., Khoo, W., Sasaki, T., Cao, Z., Penninger, J. M., Paige, C. J., Lacey, D. L., Dunstan, C. R., Boyle, W. J., Goeddel, D. V., and Mak, T. W. (1999) *Genes Dev.* **13**, 1015–1024
33. Naito, A., Azuma, S., Tanaka, S., Miyazaki, T., Takaki, S., Takatsu, K., Nakao, K., Nakamura, K., Katsuki, M., Yamamoto, T., and Inoue, J. (1999) *Genes Cells* **4**, 353–362
34. Dempsey, P. W., Doyle, S. E., He, J. Q., and Cheng, G. (2003) *Cytokine Growth Factor Rev.* **14**, 193–209
35. Yamaguchi, K., Shirakabe, K., Shibuya, H., Irie, K., Oishi, I., Ueno, N., Taniguchi, T., Nishida, E., and Matsumoto, K. (1995) *Science* **27**, 2008–2011
36. Ninomiya-Tsuji, J., Kishimoto, K., Hiyama, A., Inoue, J., Cao, Z., and Matsumoto, K. (1999) *Nature* **398**, 252–256
37. Irie, T., Muta, T., and Takeshige, K. (2000) *FEBS Lett.* **467**, 160–164
38. Mizukami, J., Takaesu, G., Akatsuka, H., Sakurai, H., Ninomiya-Tsuji, J., Matsumoto, K., and Sakurai, N. (2002) *Mol. Cell. Biol.* **22**, 992–1000
39. Ishitani, T., Takaesu, G., Ninomiya-Tsuji, J., Shibuya, H., Gaynor, R. B., and Matsumoto, K. (2003) *EMBO J.* **22**, 6277–6288

AQ: H

AQ: I

40. Itoh, K., Udagawa, N., Katagiri, T., Iemura, S., Ueno, N., Yasuda, H., Higashio, K., W. Quinn, J. M., Gillespie, M. T., Martin, T. J., Suda, T., and Takahashi, N. (2001) *Endocrinology* **142**, 3656–3662
41. Takayanagi, H., Kim, S., Koga, T., Nishina, H., Isshiki, M., Yoshida, H., Saiura, A., Isobe, M., Yokochi, T., Inoue, J., Wagner, E. F., Mak, T. W., Kodama, T., and Taniguchi, T. (2002) *Dev. Cell* **3**, 889–901
42. Matsumoto, M., Sudo, T., Saito, T., Osada, H., and Tsujimoto, M. (2000) *J. Biol. Chem.* **275**, 31155–31161
43. Li, X., Udagawa, N., Itoh, K., Suda, K., Murase, Y., Nishihara, T., Suda, T., and Takahashi, N. (2000) *Endocrinology* **143**, 3105–3113
44. Rosenberg, D., Groussin, L., Jullian, E., Perlemoine, K., Bertagna, X., and Bertherat, J. (2002) *Ann. N. Y. Acad. Sci.* **968**, 65–74
45. Schmitt, J. M., and Stork, P. J. (2002) *Mol. Cell* **9**, 85–94
46. Iwahashi, H., Takeshita, A., and Hanazawa, S. (2000) *J. Immunol.* **164**, 5403–5408
47. Kishimoto, K., Matsumoto, K., and Ninomiya-Tsuji, J. (2000) *J. Biol. Chem.* **275**, 7359–7364
48. Takaesu, G., Surabhi, R. M., Park, K.-J., Ninomiya-Tsuji, J., Matsumoto, K., and Gaynor, R. B. (2003) *J. Mol. Biol.* **326**, 105–115
49. Takaesu, G., Kishida, S., Hiyama, A., Yamaguchi, K., Shibuya, H., Irie, K., Ninomiya-Tsuji, J., and Matsumoto, K. (2000) *Mol. Cell* **5**, 649–658
50. Cheung, P. C., Nebreda, A. R., and Cohen, P. (2004) *Biochem. J.* **378**, 27–34
51. Akira, S., Takeda, K., and Kaisho, T. (2001) *Nat. Immun.* **2**, 675–680
52. Yamamoto, M., Sato, S., Hemmi, H., Hoshino, K., Kaisho, T., Sanjo, H., Takeuchi, O., Sugiyama, M., Okabe, M., Takeda, K., and Akira, S. (2003) *Science* **301**, 640–643
53. McCoy, J. M., Wicks, J. R., and Audoly, L. P. (2002) *J. Clin. Investig.* **110**, 651–658
54. Isumi, Y., Minamino, N., Kubo, A., Nishimoto, N., Yoshizaki, K., Yoshioka, M., Kangawa, K., and Matsuo, H. (1998) *Biochem. Biophys. Res. Commun.* **244**, 325–331
55. Tang, Y., Feng, Y., and Wang, X. (1998) *J. Neuroimmunol.* **84**, 207–212

AQ: J

ASBMB

The Journal of International Medical Research
2004; 32: 284 – 291

Detection of Grb-2-related Adaptor Protein Gene (*GRAP*) and Peptide Molecule in Salivary Glands of MRL/*lpr* Mice and Patients with Sjögren's Syndrome

H SHIRAIWA[1,4], M TAKEI[1], T YOSHIKAWA[5], T AZUMA[1], M KATO[6], K MITAMURA[1], T UEKI[2], A KIDA[3], T HORIE[1], N SEKI[6] AND S SAWADA[1,4]

[1]First Department of Internal Medicine, [2]Department of Dentistry and Oral Surgery and [3]Department of Otolaryngology, Nihon University School of Medicine, Tokyo, Japan; [4]Department of Internal Medicine, Nerima Hikarigaoka Nihon University Hospital, Tokyo, Japan; [5]Discovery Technology Laboratory, Research and Development Division, Mitsubishi Pharma Corp., Kanagawa, Japan; [6]Department of Functional Genomics, Chiba University, Graduate School of Medicine, Chiba, Japan

The pathogenesis of Sjögren's syndrome (SS) is poorly understood. In this study we used an in-house mouse spleen cDNA microarray to analyse genes in spleens from MRL/*lpr* (an SS mouse model) mice. We have previously demonstrated that *GRAP* genes were up-regulated in salivary glands of the same mice. The microarray analysis showed that seven out of 2304 genes were highly expressed in spleens from the MRL/*lpr* mice, one of which was the *GRAP* gene. In other words, the *GRAP* gene is highly expressed in the salivary glands and spleen of MRL/*lpr* mice. We also carried out immunohistochemical studies. Mouse and human Grb-2-related adaptor protein (*GRAP*) antigens were expressed on ductal cells and infiltrating lymphocytes in salivary glands of MRL/*lpr* mice and SS patients, but only weakly in controls (MRL/+ mice and individuals with salivary cysts). These results suggest that the *GRAP* gene might have a role in the pathogenesis of SS.

KEY WORDS: SJÖGREN'S SYNDROME, MRL/*lpr* MICE, IN-HOUSE cDNA MICROARRAY, *GRAP* GENE

Introduction

Sjögren's syndrome (SS) is a chronic autoimmune disease characterized by progressive lymphocytic infiltration and destruction of exocrine glands, such as the salivary and lacrimal glands. The lymphocytic infiltrate contains predominantly CD4+ T-cells and some B-cells including plasma cells. Dryness of the eyes and mouth is the most typical feature. It either occurs as an isolated disorder (primary form), or more often in association with another autoimmune disease (secondary form).[1–4]

The mechanism of onset and progression of

SS has been poorly understood. It has been proposed that a combination of immunological, genetic and environmental factors may play an important role in the aetiology of SS, but there remains considerable controversy. Many attempts have been made to investigate different aspects of SS. The animal model is one of the most effective approaches to studying the pathogenesis of SS, and several mouse models, such as NFS/*sld*[5,6] and MRL/*lpr* mice,[7-9] have been generated.

The MRL/*lpr* mouse is the classic murine model of autoimmune disorders, and spontaneously develops massive lymphadenopathy, arthritis, vasculitis and nephritis. It develops a disease serologically, pathologically and symptomatically similar to human SS. Significant inflammatory changes develop in the salivary glands between 12 and 16 weeks of age.[7-9] MRL/*lpr* mice have a defect in the *Fas* antigen gene which codes a critical molecule mediating apoptosis.

To understand the mechanism of onset and progression of SS, it is necessary to identify SS-related genes. To clarify the heterogeneity of gene expression in patients with SS, we began by investigating genes up-regulated in the SS mouse model.[10] We demonstrated increased expression of two genes – *IL-16* and *GRAP* – in the salivary glands of MRL/*lpr* mice using an in-house mouse spleen cDNA microarray.[10] The aim of the present study was to investigate gene expression in the spleen of the SS mouse model using a spleen cDNA microarray generated in-house. We also studied the tissue localization (using immunohistochemical staining) of Grb-2-related adaptor protein (GRAP) molecules in specimens obtained from the SS mouse model, and a human homologue of GRAP in specimens from patients with SS.

The *GRAP* genes are apoptosis-related genes, and their possible role in the pathogenesis of organ-specific autoimmune lesions in SS is discussed in light of the findings of our study.

Subjects and methods

SJÖGREN'S SYNDROME MODEL MICE

Sixteen-week-old MRL/MpJ-*lpr*/*lpr* (MRL/*lpr*) female mice (a model mouse for SS) and 16-week-old MRL/MpJ-+/+ (MRL/+) female congenic control mice were obtained from Japan SLC, Inc. (Hamamatsu, Japan). They were kept under standard conditions, according to the guidelines adopted by the Centre for Animal Experimentation, Nihon University School of Medicine, for 1 week and killed by cervical dislocation. The spleens were quickly removed, frozen in liquid nitrogen, and stored at –80 °C until use.

The ethics review committees for animal experimentation of the participating institutions approved the experimental protocol.

PREPARATION OF mRNA

Total RNA was prepared from spleens of all mice using a TRIzol® reagent (Life Technologies, Rockville, MD, USA). Subsequent cleanup was carried out using an RNeasy Maxi kit® (Qiagen, Germany) according to the manufacturer's instructions. mRNA was obtained from the total RNA using an Oligotex-dT30 mRNA purification kit® (TaKaRa Shuzo Co., Kyoto, Japan). The purified mRNA was subjected to our routine quality control procedure using formaldehyde agarose gels.

PREPARATION OF THE cDNA MICROARRAY

We constructed a cDNA microarray of mouse spleen chips in-house. It consisted of 2304 cDNAs derived from a mouse spleen library (2256 clones). This library was subjected to the oligo-capping method and cDNAs were prepared as described previously.[11,12]

Briefly, 2 mg/ml of polymerase chain reaction products, obtained by amplifying

the spleen library using universal primers, was mixed in a 1:1 ratio with 4 mg/ml nitrocellulose on dimethyl sulphoxide (DMSO)-coated glass slides (Nisshinbo, Chiba, Japan) using a robotic (SPBIO-2000®, Hitachi Software Engineering Co., Yokohama, Japan). This array includes cDNAs of housekeeping genes, such as human β-actin and glyceraldehyde-3-phosphate dehydrogenase, as internal controls, the *luciferase* gene from *Photinus pyralis* as a positive control, and human Cot I DNA as a negative control.[13]

MICROARRAY PROCEDURES

The microarray was hybridized with cDNA probes prepared from a 2-mg mRNA sample from the salivary glands or spleen of diseased and their congenic mice, and labelled with Cy3 fluorochrome (red) and Cy5 fluorochrome (green), respectively. cDNA probes were mixed, applied to the cDNA microarray, and incubated at 65 °C overnight in humid conditions. The fluorescent signals from the hybridized microarray were scanned with a fluorescent laser confocal slide scanner (ScanArray 4000®, GSI Lumonics, Ottawa, Canada). Background subtraction and normalization of the results of all arrayed genes were carried out in each spot using the QuantArray® cDNAmicroarray analysis software software (GSI Lumonics, Ottawa, Canada).

Genes showing a high fluorescence intensity (over 1.5 fold compared with control) in MRL/*lpr* mice were considered to be differentially expressed genes. The DNA sequences from the positive spots were reanalysed to confirm their accordance with our library database.

CRITERIA FOR SELECTING SJÖGREN'S SYNDROME-RELATED GENES

We selected the candidate genes that appeared more than four times in six microarray hybridization analyses. Genes that showed a high fluorescence intensity (over 1.5 fold compared with control) in MRL/*lpr* mice were considered as SS-related genes.

COLLECTION OF HUMAN SPECIMENS

Patients with SS and individuals with salivary cysts, recruited from Nihon University Hospital, participated in this study. All patients fulfilled the criteria for a diagnosis of SS as defined by the European Community Study Group on Diagnostic Criteria for Sjogren's Syndrome as a Preparatory Activity sponsored by the Directorate General for Science, Research and Development of the Commission of European Community.[14] The minor labial submucosal salivary gland specimens were taken from the lower lip. Informed consent was obtained prior to taking the biopsy.

IMMUNOHISTOCHEMICAL STAINING

Mouse specimens

Organs removed from the mice were fixed with 10% phosphate-buffered formalin and embedded in paraffin. Mouse salivary gland sections were fixed in 50% acetone at 4 °C for 30 s, then in 100% acetone at 4 °C for 5 min. Endogenous peroxidase activity was quenched with 0.3% H_2O_2 in Tris-buffered saline (TBS; 5 mM Tris–HCl, pH 7.5, 145 mM NaCl) for 5 min and non-specific staining was blocked by incubation with 10% normal mouse serum for 10 min at room temperature. The rabbit affinity purified immunoglobulin G anti-mouse GRAP peptide antibody, which was made specially for this study by Tanpaku Seisei Co. (Takasaki, Japan), was used diluted 1:100 as a primary antibody. The sections were incubated with the diluted primary antibody overnight at 4 °C, rinsed in TBS for 10 min, and incubated

with EnVision® (Peroxidase Rabbit, DAKO, Denmark) for 30 min. This was followed by additional rinsing in TBS, and incubation with a solution containing 10 mg of 3-amino-9-ethyl-carbazol in 50 ml of 0.02 M sodium acetate (pH 5.5) for 10 min and 4 ml of 30% H_2O_2 for 15 min. The sections were then rinsed in TBS, counterstained with Mayer's haematoxylin for 1 min, and mounted with an aqueous mounting medium.

Human specimens

Human salivary gland sections were processed as described for the mouse specimens, except that 10% normal pig serum was used for blocking non-specific staining. The rabbit affinity purified immunoglobulin G anti-human GRAP peptide antibody was prepared (Tanpaku Seisei Co., Takasaki, Japan) and used as described above.

Results

Five patients with SS and four with salivary cysts were involved in the study. Three MRL/*lpr* mice and three MRL/+ mice were also used.

cDNA MICROARRAY ANALYSIS

To analyse the overall gene expression in SS, we carried out cDNA microarray analysis. We identified seven SS-related genes in the spleens of MRL/*lpr* mice compared with those of MRL/+ mice using the mouse spleen cDNA microarray chip (Table 1).[11]

IMMUNOHISTOCHEMICAL STAINING

The *GRAP* gene showed increased expression in spleens of mice by spleen microarray analysis. Immunohistochemical staining revealed substantial differences between the SS model and control mice in the expression of mouse GRAP (Fig. 1).

Immunohistochemical staining of specimens from patients with SS and individuals with salivary cysts indicated that the human homologue of GRAP was expressed on ductal cells and on certain infiltrating cells in the SS patients, but only weakly in the controls (Fig. 2).

Discussion

Sjögren's syndrome is an autoimmune disease characterized by massive infiltration of lymphocytes into exocrine glands such as salivary and lacrimal glands, and the

TABLE 1
The seven genes with increased levels of expression in the spleen of Sjögren's syndrome (SS) model mice identified by cDNA microarray analysis

Accession No.	Gene	Ratio[a]
U88682	Mouse anti-DNA antibody heavy chain variable region mRNA	2.88
XM_134565	Mouse similar to Gag-Pol polyprotein mRNA	1.93
M16072	Mouse Ig active gamma-2a H-chain V-Dsp2.2-J2-C mRNA	1.64
BC036286	Mouse myeloid/lymphoid or mixed-lineage leukaemia 5, mRNA	2.17
NM_025408	Mouse phytoceramidase, alkaline mRNA	3.23
X76772	Mouse mRNA for ribosomal protein S3	1.56
NM_027817	Mouse GRB2-related adaptor protein (*GRAP*), mRNA	2.82

[a]The averages of fold change based on the normalized microarray fluorescent data of diseased (SS model) mice compared with control mice ($n = 6$).

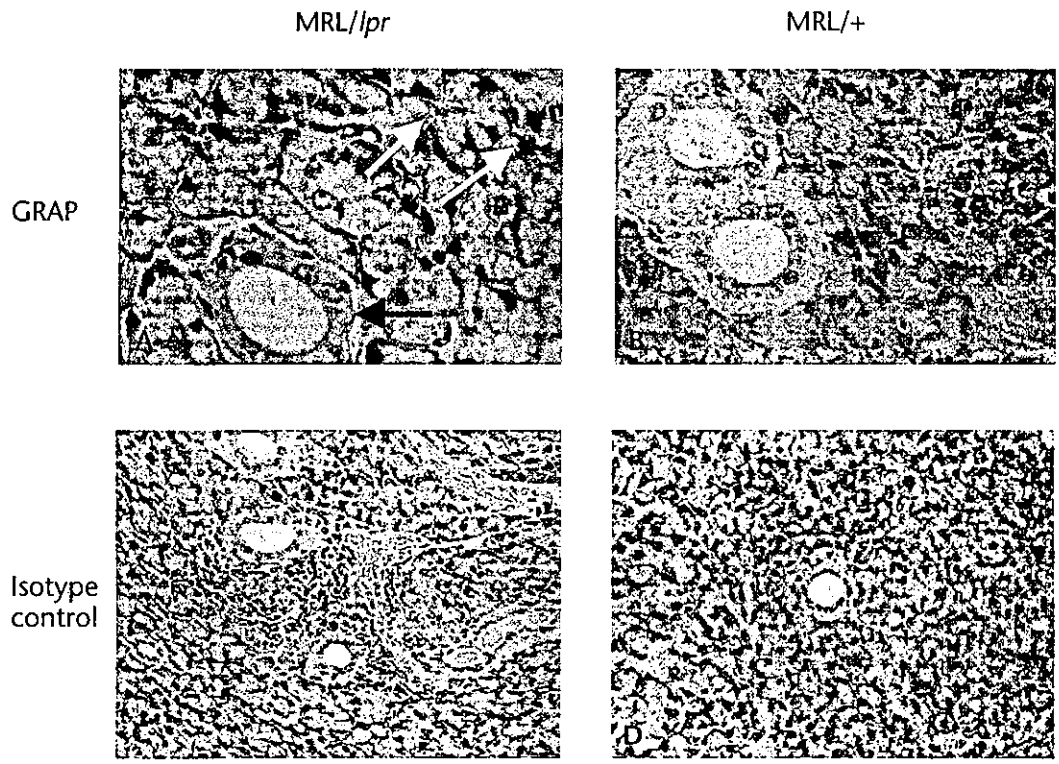

FIGURE 1: Immunohistochemically stained sections from salivary glands of MRL/*lpr* (A) and MRL/+ (B) mice. Expression of GRAP is shown in red. A substantial difference in staining intensity between the diseased (MRL/*lpr*) mice and controls (MRL/+) could be observed. The black arrow indicates ductal cells; white arrows indicate infiltrating cells. The specificity of the GRAP antibody was confirmed by normal rabbit serum immunoglobulin G, an irrelevant antibody (C, D)

subsequent destruction of these glands. Like other autoimmune diseases, the aetiology of SS remains unclear, but previous studies suggest the involvement of hereditary and environmental factors in the onset and progression of the disease. The disease is usually benign and many patients have a normal lifespan. The most common symptoms, dry eyes and dry mouth, however, are problematic and profoundly influence quality of life. In addition to these relatively benign manifestations, abnormalities of more vital organs such as renal tubular acidosis, interstitial pulmonary fibrosis and central nervous system involvement have been demonstrated.[1-4] It is therefore of importance to determine the causes of SS for better disease management.

The animal model is one of the most useful tools in the study of the pathogenesis of SS. The MRL/*lpr* mouse, a mouse model for SS, carries the *lpr* genetic defect, a mutation of the *Fas* gene, and spontaneously develops general lymphadenopathy, glomerulonephritis, systemic vasculitis and sialadenitis.[7-9] These mice are characterized by the presence of high amounts of circulating autoantibodies, such as rheumatoid factor, anti-dsDNA antibodies and immune complexes reminiscent of human systemic lupus erythematosus and rheumatoid arthritis. The onset and extent of disease in these mice are

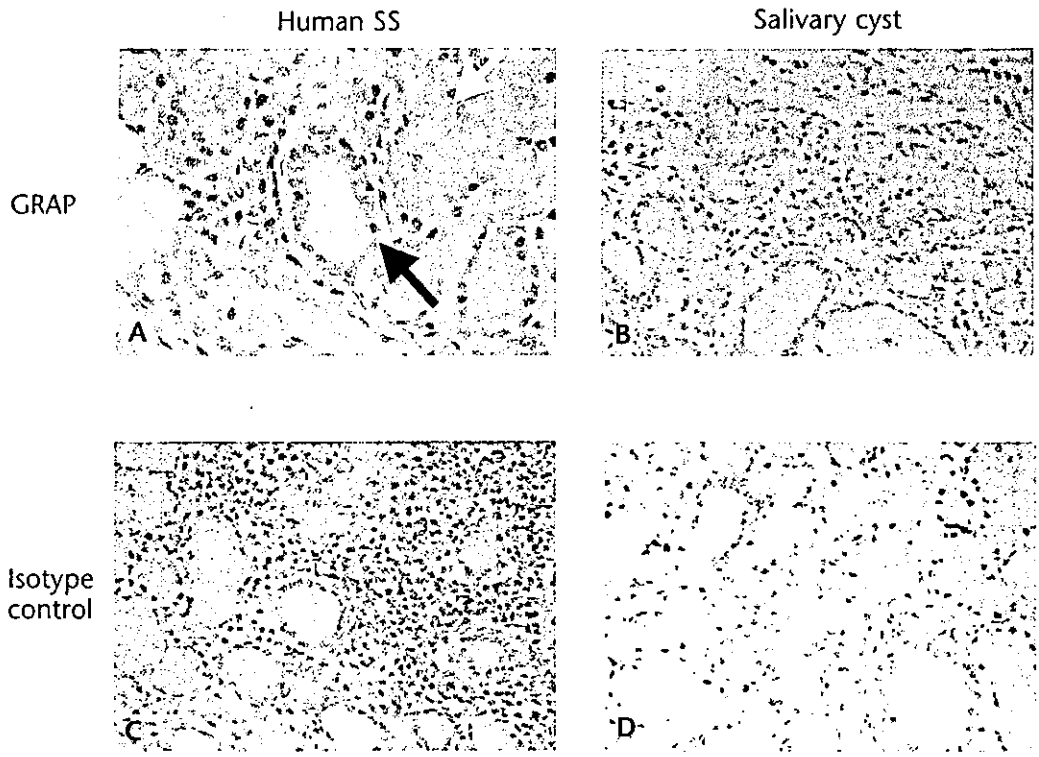

FIGURE 2: Immunohistochemically stained sections from labial salivary gland specimens obtained from patients with Sjögren's syndrome (SS) (A) and those with salivary cysts (B). Expression of GRAP is shown in red. A substantial difference in staining intensity between specimens from SS patients and salivary cysts can be seen. The black arrow indicates ductal cells; the white arrow indicates infiltrating cells. The specificity of the GRAP antibody was confirmed by normal rabbit serum immunoglobulin G, an irrelevant antibody (C, D)

also influenced by other genes, even if the basic genetic abnormality depends on the *lpr* mutation.

To identify SS-related genes, we constructed in-house cDNA microarrays based on mouse spleen cDNA libraries, and carried out cDNA microarray analysis using MRL/*lpr* mice. Up-regulation of *GRAP* genes was identified in the SS mouse model by the mouse spleen cDNA microarray analysis. The *GRAP* gene may contribute to the development of symptoms or the progression of SS.

In the mouse spleen cDNA microarray, three *Fas*-related genes (*DAXX*, *Fas*-antigen and *Fas*-associated protein) were mounted. In the present study, the expression of these three genes (*DAXX* gene, accession no. AF100956; mouse *Fas*-antigen mRNA, accession no. M83649; and mouse Mort 1 *Fas*-associated protein mRNA, accession no. M83649) was almost the same in MRL/*lpr* and MRL/+ mice. In addition, the mouse spleen cDNA microarray includes 10 genes that are obviously linked to T-cells. These genes tend to be highly expressed in the MRL/*lpr* mice compared with the MRL/+ mice. They did not strictly fulfil our criteria, thus we could not consider these as up-regulated genes.

GRAP is one of the adaptor molecules which effectively deliver signals from the immune cell surface to a down-stream functional molecule. GRAP has a structural arrangement of an SH3–SH2–SH3 domain, which is similar to other

immune cell adaptor molecules such as Grb2, GADS and GRAP2.[15,16,17] GRAP is known to be specifically expressed in lymphoid tissues, and structurally resembles Grb2 more than other Grb2 family molecules in that GRAP does not have the proline-rich motif. By immune cell activation, GRAP binds to phosphorylated tyrosine of the local area transport (LAT) at its SH2 region, and further binds to *Son of sevenless* in a way similar to Grb2. Further downstream events remain unknown. In our study, expression of the *GRAP* gene in the salivary glands of the SS mice was higher than that of the control mice. These results suggest that in diseased salivary glands and spleen, enhanced stimulation of the T-cell receptor augments signal transduction to downstream molecules associated with apoptosis. Further detailed analysis of the Grb2 family may clarify the regulation of T-cell differentiation and apoptosis in SS.

Our study provides a strategy to sort out genes that are linked to cell death or T-cell differentiation in SS using the cDNA microarray system. Moreover, our study demonstrates that the *GRAP* gene might be one of the most important SS-related genes participating in the predation and digestion of dead cells after apoptosis. In addition to the cDNA microarray analysis, we also carried out immunohistochemical analysis and demonstrated increased GRAP protein expression in the salivary glands from patients with SS. We found that GRAP was expressed on ductal cells and some infiltrating cells. Because GRAP is an apoptosis-related molecule, GRAP up-regulation might be found in the ductal cells and some infiltrating cells where apoptosis was seen to be present.

These findings also suggest that another pathway for apoptosis, such as the mitogen-activated protein kinase-mediated pathway, exists in SS besides the *Fas/Fas* ligand pathway.

Most recently, Winer *et al.*[18] reported a new autoantigen, ICA69, that may play an important role in the progression of the disease in another primary SS mouse model – the non-obese diabetic mouse. ICA69 cDNA was not mounted on the cDNA chip in our study, but it would be of interest to examine the expression of the *ICA69* gene in MRL/*lpr* mice using our microarray system. Further analysis of the candidate genes identified in this study and SS-related molecules like ICA69 will help clarify the pathogenesis of SS.

Acknowledgements

We are grateful to Dr Ronsuke Suenaga and Dr Shigeyoshi Fujiwara (National Centre for Child Health and Development) for valuable constructs and to Kumiko Takeshita for technical assistance.

• Received for publication 27 October 2003 • Accepted subject to revision 8 November 2003
• Revised accepted 15 January 2004

Copyright © 2004 Cambridge Medical Publications

References

1 Talal N, Sokoloff L, Barth WF: Extrasalivary lymphoid abnormalities in Sjögren's syndrome (reticulum cell sarcoma, 'pseudolymphoma', macroglobulinemia). *Am J Med* 1967; 43: 50 – 65.
2 Hoffman RW, Alspaugh MA, Waggle KS, Durham JB, Walker SE: Sjögren's syndrome in MRL/*lpr* and MRL/n mice. *Arthritis Rheum* 1984; 27: 157 – 165.
3 Moutsopoulous HM, Fauci AS: Immunoregulation in Sjögren's syndrome: influence of serum factors on T-cell subpopulations. *J Clin Invest* 1980; 65: 519 – 528.
4 Fox RI: Clinical feature, pathogenesis, and treatment of Sjögren's syndrome. *Curr Opin Rheumatol* 1996; 8: 438 – 445.
5 Haneji N, Hamano H, Yanagi K, Hayashi Y: A new animal model for primary Sjögren's syndrome in NFS/sld mutant mice. *J Immunol* 1994; 153: 2769 – 2777.